5 CATCHMENT HYDROLOGY UNDER FUTURE CLIMATE SCENARIOS

Ciaran Broderick and Conor Murphy

5.1 Introduction

On every scale, changes in climate are likely to have significant impacts on freshwater hydrology, with increased energy resulting in an intensified hydrological cycle. Given the complex and fragile interaction between the climate system and land-surface hydrology, any changes in the primary processes of precipitation and evaporation will have considerable knock on effects for the rest of the hydrological cycle. In examining the implications of climate change for catchment hydrology in Ireland, Murphy and Charlton (2008) highlight that the potential impacts of climate change on hydrology and water resources are diverse and complex, while each catchments individual characteristics play a pivotal role in determining the hydrological response to climate change. This is in line with findings from Prudhomme and Davies (2009) who found that, for the UK, results of climate change impact assessments are catchment-specific and implies the necessity of a full modelling exercise when major planning and policy decisions are to be made. Despite results being catchment specific, a number of general conclusions can be made from the work of Murphy and Charlton (2009) in the wider Irish context;

- Reductions in streamflow are likely for the summer and autumn months in the majority of catchments, while greatest increases are suggested for winter. However, large differences exist in the magnitude of change simulated between catchments even when using the same future climate scenarios.
- The seasonality of streamflow is also likely to increase, with higher flows projected in winter and spring, while extended dry periods are suggested for summer and autumn in the majority of catchments.
- In relation to extremes the frequency of both high and low flows is likely to increase.

Such changes in freshwater hydrology are likely to have considerable implications for the distribution and abundance of key fish species where populations are influenced strongly by their habitat, which includes a range of biotic and abiotic factors that have complex interactions (Walsh and Kilsby, 2007). This is especially true for the Atlantic salmon, which is increasingly being recognised as of value, not just as a target species for fisheries but also for

conservation on grounds of biodiversity and as an indicator of environmental health (Winfield et al., 2004). In line with the importance of this species, it is now protected under the European Union Habitat Directive and is likely to be used extensively as a 'sensitive species' in the context of the European Water Framework Directive (Walsh and Kilsby, 2007).

In relation to climate change, Walsh and Kilsby (2007) highlight that changes in the flow regimes of the freshwater environment could have impacts for all life stages of Atlantic salmon; during spawning and egg deposition increases in flooding has the potential to wash out eggs laid in gravels, while decreased flows could leave redds stranded preventing the emergence of fry. The authors also highlight that wetter springs may induce earlier migration of smolts to sea, decreasing subsequent survival rates, while for juvenile salmon the increased risk of successive low flow years may have detrimental effects on salmon stocks, taking years to recover (Walsh and Kilsby. 2007).

The importance of understanding the local impacts of climate change is emphasised by Friedland et al. (2009) who highlight that during their freshwater stage salmon are locally adapted and in some contexts, an individual river stock needs to be viewed and managed as a species (Taylor, 1991). Projections of climate change over the next century suggest that temperature increases over land will exceed those expected over the surface of the oceans (Boer et al., 2000). In this context, we may look to changes in the marine environment as the forcing factor controlling stock complexity and productivity, but the changing state of conditions in fresh water may be the more important factor controlling species distribution and viability (Friedland et al., 2009). Understanding the likely impacts of climate change on catchment hydrology is critical in order to examine the sensitivity of key species and to enhance our ability to conserve and manage the viability and diversity of the species in Irish waters. This chapter examines the likely changes in the monthly flow regime and extreme hydrological events for the Burrishoole catchment.

5.2   Research Design

In order to increase the information content of simulations and fully exploit the richness of observations available, the catchment was sub-divided into constituent sub-catchments, with each being modelled independently. In line with the objective of quantifying uncertainties in future simulations of catchment hydrology, the climate scenarios developed in Chapter 4 were used as input to a suite of rainfall runoff models, trained to represent the hydrological behaviour of each catchment, for the coming century. In maintaining the priority of quantifying uncertainty in future projections the uncertainty derived from the use of different rainfall-

runoff models and the parameter uncertainties that emerge in applying the models were quantified. Three future time periods, of thirty years duration, were employed for the analysis of future changes in catchment hydrology; the 2020s (2010-39), the 2050s (2040-69) and the 2080s (2070-99). Changes in the monthly flow regime, the frequency and duration of low flow events and the frequency of flood events for each future period were calculated relative to the simulated control (or reference) period of 1961-1990. Natural variability in the hydrological regime of each sub-catchment was also quantified to assess the significance of future changes driven by climate change.

5.3   Catchments and Datasets

5.3.1   Catchments Modelled

This study was undertaken on five sub-catchments which comprise part of the greater Burrishoole catchment system (84 km2). In addition, the Glendahurk, a much smaller catchment system which borders the Burrishoole catchment to the west, was also considered. Figure 5.1 outlines the catchments modelled and their key characteristics. The Burrishoole catchment itself lies in a North-South direction at the Northeast corner of Clew Bay where it drains into the Atlantic. The catchment is located at the heart of the Nephin Beg Mountain.
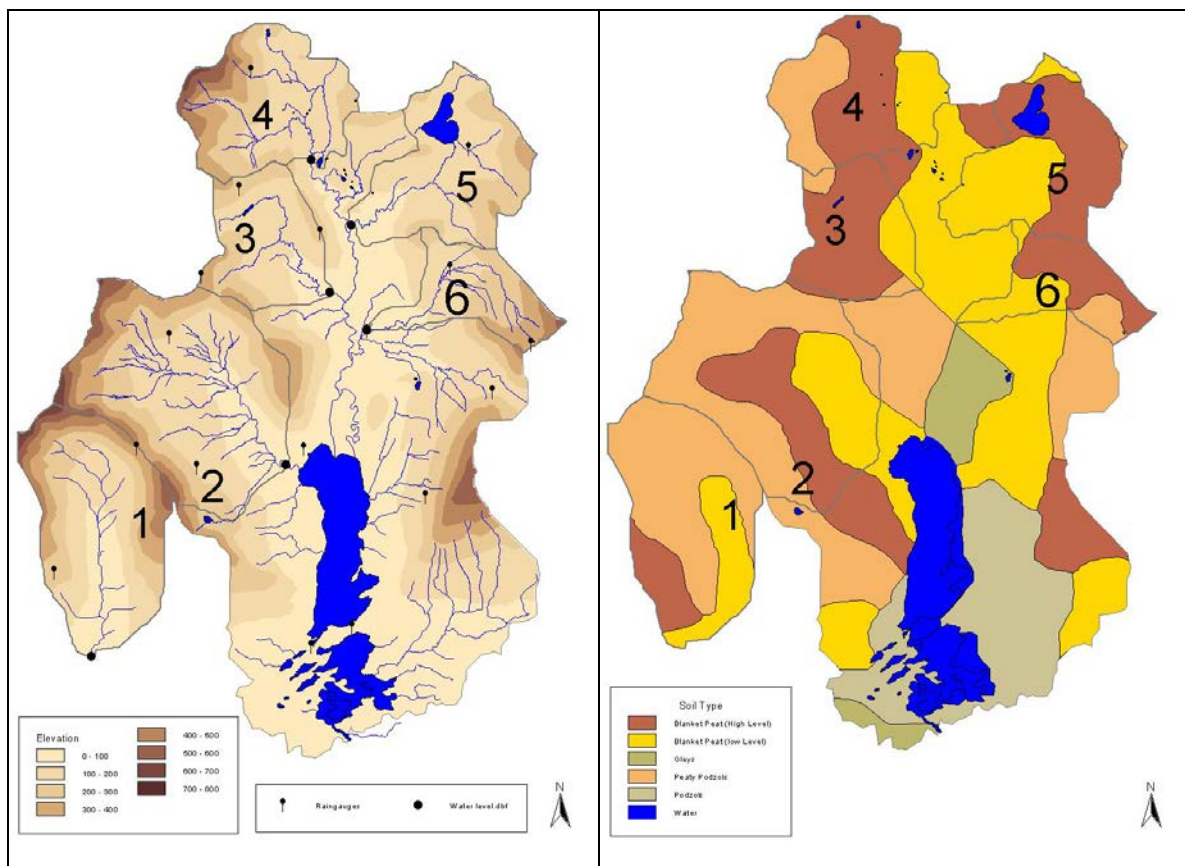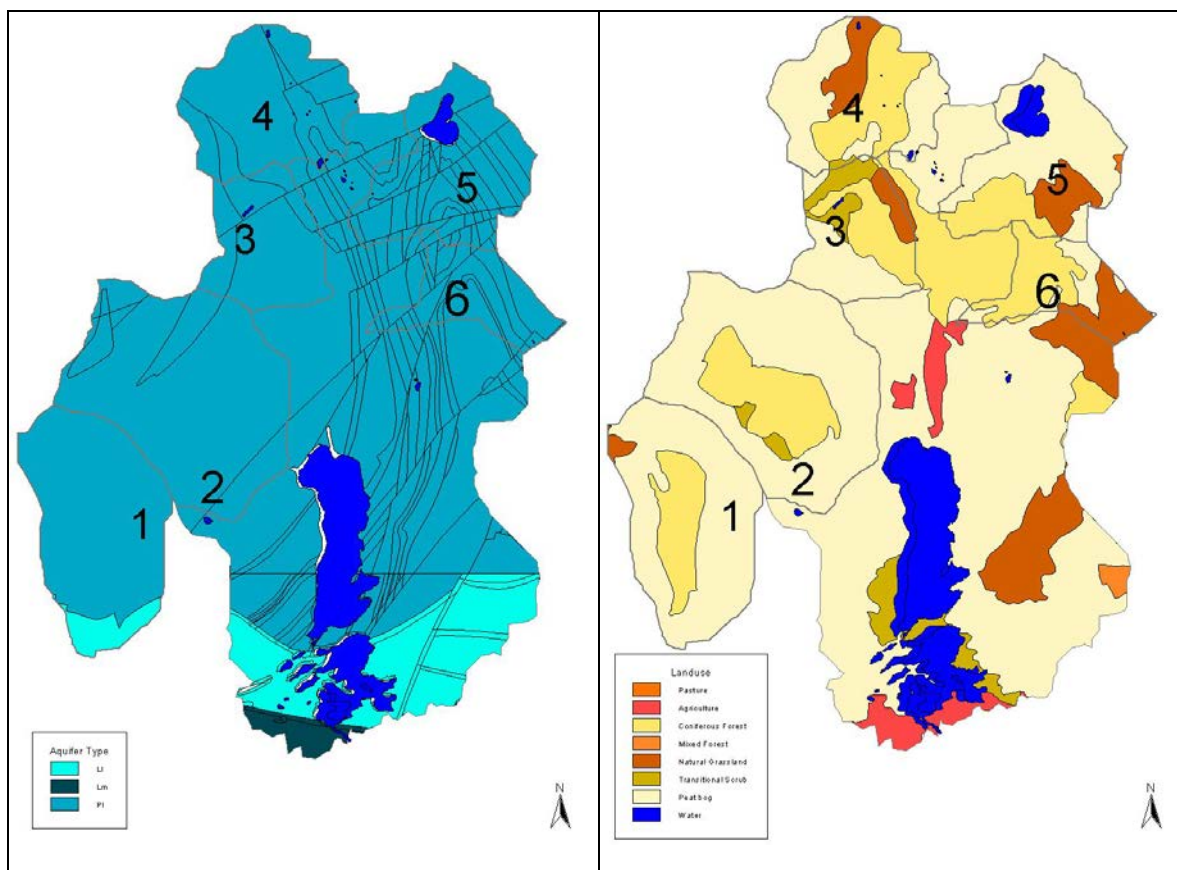
Figure 5.1 The Burrishoole catchment and sub-catchments modelled (1.Glendahurk, 2.Glenamong, 3.Maumaratta, 4.Altahoney, 5.Goulan, 6.Srahrevagh). Maps represent catchment elevation and the location of river level and precipitation gauges (top left), soil type (top right), aquifer type (bottom left) and landuse (bottom right).

Range and takes on an amphitheatre like shape with steep slopes to the north, west and east delineating the drainage boundary. The surrounding terrain is complex being characterised by localised valleys, steeply sloping mountain ranges and rapid changes in elevation. The altitudinal range for the catchment spans 700 metres, from 10m at the outlet point to 710m at the highest peak on the contributing upland areas. The Burrishoole system includes three main lakes, the brackish Lough Furnace (1.41 km2) as well as Loughs Feeagh (4.1 km2) and Bunaveela (0.54 km2), both of which are freshwater lakes. Lough Furnace and Lough Feeagh are situated in the lower part of the Burrishoole valley whilst Bunaveela is located in the upper reaches of the Goulan sub-catchment. The catchment system has a dense drainage network comprised of at least 70 km of rivers and streams (Poole, 1994).

The five main constituent sub-catchments of the Burrishoole system were selected for analysis in this study. Included were the Glenamong, Maurmatta and Altahoney located in the west and north-west parts of the catchment. Also selected were the Goulan and Srahrevagh sub-catchments situated in the north-eastern and eastern parts of the catchment. Each of these catchment systems, either directly or through the drainage network, feed into the two lakes situated on the valley floor. The additional catchment considered (Glendahurk) lies adjacent to

the Glenamong sub-catchment and is a completely independent system, forming a tributary of the Owengarve River which flows directly into Clew Bay.

Each catchment displays relatively similar properties in terms of their land cover, soil type, groundwater capacity and morphometric attributes (e.g. basin slope, area and shape). Of each catchment considered the Glenamong, with an area of 17.2 km2, is the largest followed by the Glendahurk (12.42 km2). The smallest catchment is the Srahrevagh which has an area of just 4.9 km2. Coniferous forests (20-45% coverage) and blanket peat bogs (40-60%) are the dominant land cover across each catchment system with small areas of natural grassland (10-20%) and transitional scrubland present (Corine, 2003). The entire area is underlain by unproductive bedrock and consequently each catchment has a relatively poor groundwater storage and transmissive capacity (GSI, 2003). The overlying soils mainly consist of blanket peat and peaty podzols (Gardiner and Radford, 1980). Peat is overwhelmingly dominant in all catchments, especially in those situated in the upper reaches of Burrishoole including the Altahoney (80% coverage), Goulan (100%) and Srahrevagh (90%) sub-catchments. The Glenamong (70%) and Glendahurk (75%) are also notable for a high proportion of blanket peat coverage. Tables 5.1 - 5.4 describe the physical attributes of each catchment including percent landuse (Table 5.1), aquifer (Table 5.2) and soil type coverage (Table 5.3) along with their respective geometric properties (Table 5.4).

Table 5.1 Percent coverage of Corine classified landuse in each sub catchment modelled.

Corine Land Cover Classification							
Code	Classification	Catchment					
		Glendahurk	Glenamong	Maurmatta	Altahoney	Goulan	Srahrevagh
312	Coniferous Forest	40	30	40	45	20	45
412	Blanket Bog	60	60	40	35	60	45
321	Natural Grassland		10	10	20	20	10
324	Transitional woodland scrub			10			

Table 5.2 Percent coverage of aquifer category in each sub catchment modelled.

Aquifer Classification							
Code	Classification	Catchment					
		Glendahurk	Glenamong	Maurmatta	Altahoney	Goulan	Srahrevagh
PL	Poor aquifer, generally unproductive except in local zones	90	100	100	100	100	100
LI	Locally important, generally moderately productive in local zones	10					

Table 5.3 Percent coverage of soil type in each sub catchment modelled.

Soil Type						
Classification	**Catchment**					
	Glendahurk	**Glenamong**	**Maurmatta**	**Altahoney**	**Goulan**	**Srahrevagh**
Blanket Peat	75	70	90	80	100	90
Peaty Podzols	25	30	10	20		10

Table 5.4 Geometric characteristics of each sub catchment modelled.

Geometric Properties						
Attribute	**Catchment**					
	Glendahurk	**Glenamong**	**Maumaratta**	**Altahoney**	**Goulan**	**Srahrevagh**
Area (km2)	12.4	17.1	6.4	9.2	9.6	4.9
Min Elevation (m)	47	12	54	94	59	23
Max Elevation (m)	710	708	383	626	389	550
Slope (°)	14	12	10	13	8.8	9

All of the selected catchments have a flow regime which is highly responsive to rainfall and exhibit behavior which is typically associated with runoff dominated systems. This is related to the geometric properties of each catchments drainage basin (e.g. steep slope, small area), and the low storage capacity of the underlying geology. Both these factors contribute to each catchments inability to attenuate the rapid movement of water through the catchment system or dampen the streamflow response to high precipitation events. The low contribution of baseflow to catchment discharge, especially during drier summer months, underlines the deficiency in groundwater capacity across all catchments. Streamflow records for two of the selected catchments showed that they had completely dried up on at least one occasion after a sustained period without rainfall. The presence of blanket peatland plays a significant role in shaping the hydrology of each catchment. It has been shown that well developed macropores and pipes which exist in the peat matrix provide an effective conduit for rapid subsurface flow. Peat covered hillslopes give rise to optimum conditions for overland flow during a storm event. Both these factors contribute to the flashy nature of storm runoff from peat dominated catchments such as those included in this study (Holden and Burt, 2003).

5.3.2   Observed Datasets

Historical records of streamflow and precipitation were taken from instrumental stations located at various points across the study area. River levels are recorded at the outlet for each catchment on a 15 minute interval time step. Average daily volumetric flow values were derived from recorded water levels using a rating curve calculated for each gauging point. Observed streamflow datasets were of varying lengths and quality with some displaying

evidence of disruption subsequent to extreme events. Table 5.5 provides some details of the streamflow records for each catchment.

Table 5.5 Data statistics for river flow record at each gauging point

Catchment	Record Start Date	Record End Date	Data (days)	Missing n (%)	Mean Daily (m3/sec)	Std. Dev (m3/sec)	95 % ile (m3/sec)
Glenamong	Jun-02	Aug-09	2398	10.1	0.928	1.172	3.258
Maumaratta	Jun-02	Aug-09	2392	10.3	0.460	0.662	1.492
Altahoney	May-02	Aug-09	2546	3.7	0.597	0.890	2.342
Srahrevagh	Jun-02	Aug-09	2419	9.3	0.320	1.848	1.032
Goulan	Apr-03	May-06	1096	5.3	0.337	0.384	1.108
Glendahurk	Jun-02	Aug-09	2125	20.4	0.183	0.290	0.714

An extensive upland rain gauge network traverses the study region with multiple gauging stations being located in each catchment. Precipitation datasets used in this study were obtained from each of these recording points. Historical records of daily precipitation were also obtained from the Millrace climatological station located close to the outlet of the Burrishoole catchment. The observed rainfall series for this station is considerably longer (1961- 2009) than those provided by the more recently established gauging points in the upper reaches of the catchment.

Owing to the complexity of the local terrain (e.g. elevation, slope, aspect) the precipitation regime varies considerably across the catchment system. For each catchment considered a weighted average rainfall series, derived using precipitation records from gauges located close to or within each catchment boundary, were employed during model development. This allowed the spatial distribution of rainfall across each catchment to be considered and addressed the problematic issue of missing values in individual datasets. Only those rainfall records which exhibited a high correlation with streamflow for a given catchment were selected. For calculation of the averaged time-series, each of the individual rainfall records considered were weighted according to the correlation they had with streamflow. Observed records for potential evaporation were obtained from the Belmullet synoptic station located north-west of the catchment. This station is operated by the Irish meteorological service Met Eireann. Table 5.6 provides statistics for the precipitation records available for use in this study.

Table 5.6 Data statistics for precipitation record at each gauging point

Precipitation Gauging Station	Record Date Start	Data (days)	Missing n (%)	Mean (mm/day)	Median (mm/day)	Std. Dev (mm/day)	95 % ile (mm/day)
Glenamong 1	May-02	1510	43.4	4.8	2.2	7.6	18.2
Glenamong 2	May-02	2397	10.2	5.4	3.0	7.7	20.4
Glenamong 3	May-02	2535	5.0	5.1	2.0	7.7	20.4
Glenamong 4	Jul-03	1925	14.4	6.5	2.6	9.4	24.7
Maumaratta	May-02	2083	21.9	5.2	2.2	7.3	20.8
Altahoney	May-02	1903	28.7	6.3	2.2	10.4	25.2
Srahrevagh 1	May-02	2505	6.1	4.4	1.6	6.9	18.8
Srahrevagh 2	May-02	2224	16.6	4.0	1.8	5.6	15.4
Srahrevagh 3	May-02	2233	16.3	4.8	1.8	7.0	19.3
Goulan	May-02	2492	6.6	5.1	2.0	7.6	20.1
Namaroon	Jan-04	1848	10.5	6.6	3.2	8.7	24.3
Glendahurk	Jun-03	1676	26.5	4.9	2.2	6.6	17.4
Millrace	Jan-61	17696	0.4	4.3	1.8	6.2	16.6

5.3.3   Future Climate Scenarios

To examine the impacts of climate change on each catchment's hydrological regime point scale estimates of precipitation and potential evaporation, for the full period 1961-2099, were derived from large-scale GCM output using statistical downscaling techniques as discussed in Chapter 4. In order to address the various factors which contribute to uncertainty in climate projections (e.g. emission scenarios, GCM structure, parameterisations and climate sensitivities) the output from three GCMs, each run using two different SRES emission scenarios (the medium-high (A2) and medium-low (B2)) were used as the input data for the downscaled series. The GCMs considered included: HadCM3 from the Hadley Centre for Climate Prediction and Research (Met Office, UK); CCGCM2, from the Canadian Centre for Climate Modelling and Analysis (CCCMA; Canada) and CSIRO-Mk2 from the Commonwealth Science and Industrial Research Organisation (CSIRO, Australia). The limitations associated with statistical downscaling represent an additional source of uncertainty in estimates of local climate change. To address this both Generalised Linear Models (GLMs) and a statistical downscaling software package (SDSM) were used to develop climate scenarios for the catchment.

The GLM approach was used only to downscale precipitation whilst SDSM was employed to produce downscaled scenarios for both precipitation and potential evaporation (PE). The GLM is a fully deterministic method and as such only one downscaled rainfall series was produced from each GCM and emission scenario. SDSM is also a regression based downscaling method;

however it incorporates an additional stochastic component which allows multiple synthetic series or realisations of future weather data to be produced using a common GCM predictor set. Each individual realisation exhibits a different time-series evolution but has the same overall statistical properties. The integration of this weather generator type module allows new temporal sequences of extreme events to be generated for future climate assessment (Diaz Nieto and Wilby, 2005) and represents an attempt to capture the 'chaotic' nature, or natural variability, of local weather conditions in the predicted series. Using SDSM an ensemble of one hundred individual sequences of daily precipitation and evaporation data for the period 1961-2099 were generated using grid-scale climate projections from each of the aforementioned GCMs. In order to assess the impacts of projected climate change on the river flow regime of each sub catchment each ensemble member, along with the deterministic scenario derived from the GLM, were used as input data for hydrological models.

5.4   Estimation of Natural Climate Variability for Baseline Conditions

Natural climate variability refers to natural fluctuations within the climate system that occur across a range of time scales from daily to multi-decadal and spatially from the regional to global scale. While a number of authors have related changes in climate variability to changes in observed records, very few have compared the effect of natural multi-decadal climate variability with human induced climate change over the coming century. Arnell (2003) conducted such as assessment for simulated changes in river flows in the UK by using climate projections from the HadCM2 model assuming no change in greenhouse gas concentrations and concluded that even by the 2050s streamflow in some seasons will be well within the range of multi-decadal climate variability, especially in groundwater dominated catchments. Furthermore, when the effects of anthropogenic climate change and natural variability are combined, the range of possible future changes increases substantially (Arnell, 2003). More recently, Prudhomme and Davies (2009) estimated natural climate variability by running a hydrological model with rainfall and PE series resampled, using block resampling from observations. Results derived by Prudhomme and Davies (2009) found that only half of the changes projected are significant within the estimated natural variability of the observed flow regime.

In estimating natural variability for the catchments modelled, a procedure similar to that of Prudhomme and Davies (2009) was employed. Given the short length of observed records in the catchments, NCEP reanalysis data was used to estimate the ranges of natural variability using an ensemble of 100 synthetic precipitation series. Each series generated was long enough

to span the period 1961-1990 as this represents the standard baseline used in climate impact assessments. The scenarios derived from grid-scale NCEP data were downscaled to the Millrace station. In order to translate this downscaled dataset to each study catchment Quantile mapping was applied. The translated NCEP dataset for each catchment was then used to calculate the natural variability of their flow regime under 'current' climate conditions. Quantile mapping is discussed below in section 5.5.

To construct each synthetic series the NCEP precipitation data was split on a seasonal basis into four sub-series (winter, spring summer and autumn). Each sub-series consisted of a sequence of 'blocks' representing observed daily values for a three month period (e.g. DJF). Resampling was carried out on a seasonal rather than monthly basis in order to preserve the annual precipitation cycle and avoid any unrealistic alteration in the catchments water budget. Individual series were generated by selecting at random one block from each of the four seasonal sub-series, respecting their sequential order (e.g. a spring block is selected after a winter block). Each seasonal block was selected independently from the preceding one to ensure that two consecutive blocks were not selected from the same year in which they were recorded. Once sampled the data was returned to the sampling pool which allowed the same block to be sampled repeatedly. This ensured that low frequency events could be represented in the same synthetic series multiple times. A rainfall runoff model (HYSIM) was used to simulate the runoff generated by each resampled member. Observed potential evaporation at Belmullet for the period 1961-1990 was used in each model run. This input variable was not resampled as it displays a strong annual cycle and exhibits little interannual variability. The combined output from all models and ensemble members provides some measure of natural variability under reference climate conditions.
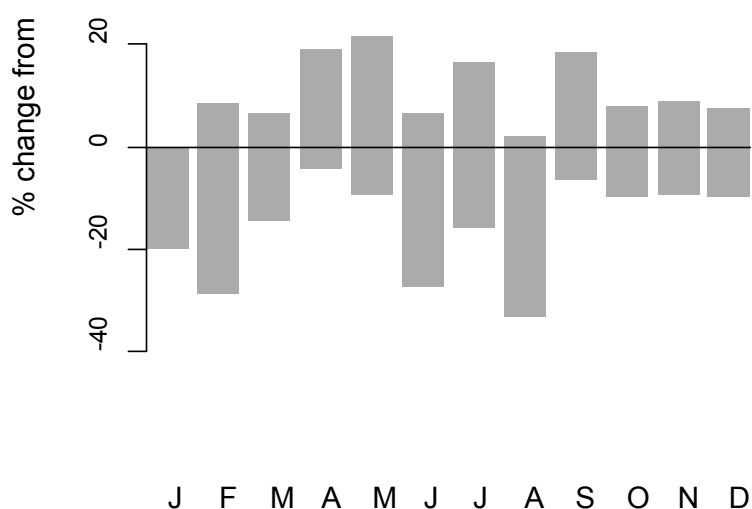

253

Figure 5.2 Natural variability bounds for the Glenamong catchment constructed through resampling of NCEP data.

Ranges for natural variability for the Glenamong catchment are shown in Figure 5.2. For most months the estimated ranges of natural variability are within plus or minus 20 percent of the 1961-1990 monthly averages. The largest bounds are evident for February, June and August, in excess of 30 percent deviation from the long term mean. Such a large range of natural variability in the flow regime is representative of the flashy response of the catchment and are consistent with ranges derived for UK catchments by Prudhomme and Davies (2009).

The natural variability ranges produced for each catchment were employed to assess the significance of future changes in the monthly flow regime for each future time period. Future changes due to climate change are only defined as significant if at least 75% of all ensemble member simulations are outside of the 90% confidence interval of the natural variability range of the reference period 1961-1990. Future changes within the range of natural variability of the baseline climate cannot be attributed to anthropogenic climate change. This is line with the approach advanced by Prudhomme and Davies (2009), who highlight that adopting the threshold of 75% is a practical choice that can be compared to 68% of values that fall within plus or minus one standard deviation around the mean and 16% of values below or above one standard deviation from the mean for a normal distribution.

5.5   Quantile Mapping of Climate Scenarios

When developing the hydrological model for each catchment, model simulations which used weighted average rainfall as their input data displayed far superior efficiency scores when compared to model runs which employed the observed precipitation record from the Millrace climatological station. This is due to the localised nature of the rainfall regime across the study area - which is to a large extent driven by the complex terrain and the strong influence of topographical features (e.g. elevation, slope, aspect). Thus, precipitation receipts at the Millrace station do not fully reflect the spatial variability of rainfall across upland areas. Ideally future precipitation scenarios would have been downscaled for each individual catchment with the aim of capturing locally specific conditions. However, due to the short records available for upland gauging points, precipitation scenarios could not be downscaled directly to these sites. Instead it was only possible to downscale rainfall scenarios to the Millrace station, for which records of the required length were available to develop downscaling models. To overcome this, quantile mapping was used to construct precipitation scenarios for each sub catchment using the point-scale precipitation datasets downscaled to the Millrace station outlined in Chapter 4.

5.6   Hydrological Modelling

5.6.1   Uncertainty in Hydrological Models

In order to translate future climate scenarios into hydrological simulations different hydrological modelling approaches were employed. Conceptual rainfall-runoff (CRR) models have been the most widely used for climate impact assessment (Cunnane and Regan, 1994; Arnell and Reynard, 1996; Sefton and Boorman, 1997; Pilling and Jones, 1999; Arnell, 2003; Charlton and Moore, 2003; Wilby, 2005; Murphy et al., 2006; Murphy and Charlton 2008; Steel Dunne et al., 2008; Prudhomme and Davies 2009). Central to the use of CRR models in climate impact assessment is their ability to characterise the catchment system as a simplified agglomeration of stores representing catchment processes, enabling such models to be applied to a wide variety of catchments in different climates. CRR models also tend to contain a small number of parameters, many of which can be measured from physical reality, while the lumped nature of such models only require parameter values on a catchment or sub-catchment scale. Consequently, simple model structures, non-linear representations of the hydrological system as well as the ability to simulate the movement and storage of water in soils have led to the widespread use of CRR models in climate impact assessment. Despite their wide application CRR models are associated with considerable uncertainty due to their simplified structure and varying degrees of complexity. Broadly speaking there are three principal sources of uncertainty in hydrological models; errors associated with input data and data for calibration, imperfection in the model structure and uncertainty in model parameters (Jin et al., 2009).

Due to their conceptual nature CRR models only reflect a particular interpretation or simplification of the hydrological system, with for example, different system processes and components being omitted, added or given a different weighting in the model structure. As a consequence not all models are the same and although they may provide an adequate representation of the system over the observed fitting period, under the same future climate forcing scenario their projections may diverge significantly. Refsgaard et al. (2006) state that although model structure is one of the key sources of uncertainty in model projections it is frequently neglected and no generic methodology exists with which to address it. They highlight the use of a scenario based approach where a number of alternative conceptual models are considered. For each of these, the model input and parameter uncertainties are considered, following from this the differences between model simulations can then be used as a measure of the uncertainty attributable to model structure. This multi-model approach has previously been applied in a flood forecasting context. Butts et al. (1993) used 10 different models to assess the uncertainty in flood projections arising from model structure. Their study suggested that exploring an ensemble of model structures provides a valuable method with

255

which to address this aspect of model uncertainty. Marshall et al. (2007) reiterate this point stating that the uncertainty arising from model structure requires developing alternatives, where the output from multiple models are combined to produce an ensemble of model simulations, the range of which provides some estimate of model structure uncertainty. The strategy of applying several alternative models, or at least the same model with a different internal set-up or architecture, is already common practice in climate modelling. Uhlenbrook et al. (1993) previously assessed the uncertainties arising from different model structures in the context of the HBV CRR model. Their study demonstrated that it is possible to obtain good efficiency scores using model structures which represent both sensible and incorrect conceptualisations of a given catchment system. This alludes to the compensatory role parameter estimates can play in concealing a poor representation of the true system in the model structure.

Addressing model uncertainty is an important aspect of climate impacts assessment and in the context of this study was considered by employing two different modelling strategies. The first employed HYSIM, a CRR model which has previously been used in the field of climate impacts analysis. The second modelling strategy implemented was based on the use of Artificial Neural Networks (ANNs). To assess model uncertainty previous studies have used the results from several different hydrological models to produce a range of equally plausible streamflow projections. The level of agreement exhibited between different models provides some indication of model uncertainty. In this study the two selected modelling techniques were firstly applied to a single catchment to determine the magnitude of inter-model uncertainty and following from this, whether the application of both models to each of the remaining catchments was necessary. The Glenamong catchment was selected as the study catchment for this analysis. To assess the relative skill of each method under observed conditions both were used to simulate streamflow for the same validation and calibration periods. In addition the agreement shown between the future simulations from each model under the same climate forcing scenario were examined.

A second key source of uncertainty associated with CRR models is that due to limitations associated with the definition of model parameters, with such models commonly associated with issues of parameter stability, parameter identifiability and equifinality, each of which gives rise to uncertainty in model output. Wilby (2006) shows that uncertainty in future flow changes due to equifinality is comparable in magnitude to the uncertainty in emissions scenario. In this study the uncertainty associated with parameter identifiability is addressed using the

Generalized Likelihood Uncertainty Estimation (GLUE) procedure. This is discussed below in the context of the CRR model employed.

5.6.2   HYSIM: a Conceptual Rainfall- Runoff Model

HYSIM (Manley, 1993) is a lumped CRR model, which uses rainfall and potential evaporation data to simulate river flow using parameters for hydrology and hydraulics that define the river basin and channels in a realistic way. HYSIM was chosen for use in this study for a number of reasons, firstly many of its parameters are physically based. Of the 17 parameters which must be set in the model most are relatable to readily measurable basin characteristics. Such a model is likely to perform well under climactic conditions more extreme than those on which it has been calibrated. The lumped nature of HYSIM was also commensurate with the relatively homogenous conditions across each catchment (e.g. soil type, geology). Furthermore the model was shown to perform well in the presence of complicating factors such the presence of peatlands and the 'flashy' nature of the selected catchments.

The model is built around two sub-routines; the first of these simulates catchment hydrology while the second simulates channel hydraulics. A complete overview of the parameters included in the model and the linkages between stores are given in Figure 5.3 below. In relation to the hydrology routine seven natural stores are represented. These include snow storage (not implemented), interception storage, from which evaporation takes place at the potential rate, the upper soil horizon, the lower soil horizon, transitional groundwater, groundwater and minor channel storage. Interception storage represents the storage of moisture by the vegetation canopy. Evaporation accounts for losses from this store. Any moisture in excess of storage, determined by vegetation type, is passed on to the upper soil horizon. The upper soil horizon represents the moisture held in the upper (A) horizon or topsoil and has a finite storage capacity equal to the depth of the A horizon multiplied by its porosity. A limit on the rate at which moisture can enter the upper soil store is applied based on its potential infiltration rate. Losses are met by evaporation, interflow and percolation to the lower soil horizon. Evaporation is controlled by the forces of capillary suction, while interflow is a function of the effective horizontal permeability of the soil layer. The lower soil horizon represents moisture below the upper horizon but still within the rooting depth of vegetation. Again evaporation and interflow account for losses from this store as well as percolation to groundwater.
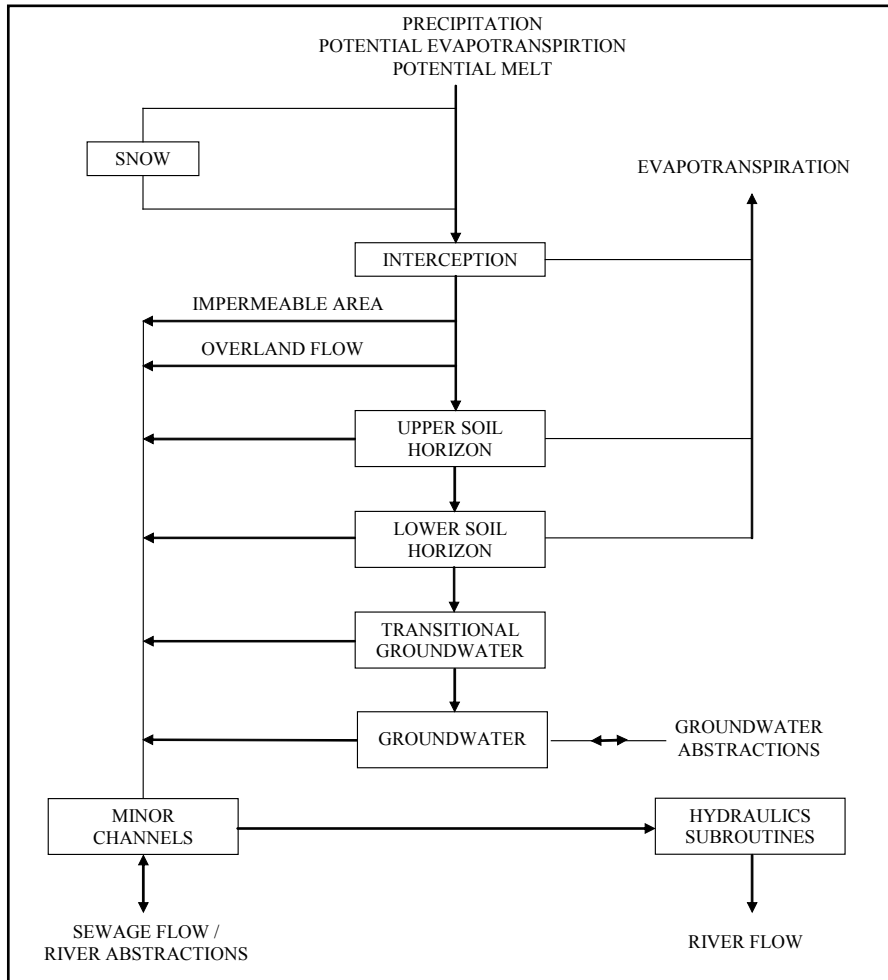
257

Figure 5.3 HYSIM model structure

The transitional groundwater store is an infinite linear reservoir, which serves to represent the first stage of groundwater storage. This store has greatest importance in catchments with permeable geologies where many of the fissures and fractures holding moisture may interact with the stream channel rather than with deeper groundwater. Losses from this store are controlled by a discharge coefficient and by the proportion of the moisture leaving storage that enters the river channel. Groundwater is also represented as an infinite linear reservoir. The final conceptual store represented by HYSIM is minor channel storage. This component represents the routing of flows in minor streams and ditches.

One of the defining features of CRR models is that a number of their parameters are not physically measurable and must be calibrated using some form of manual or automatic optimization procedure. Model calibration involves iteratively altering the models effective parameter values with the aim of minimising deviations between model simulations and observed streamflow from the selected catchment. These parameters represent important physical processes in the catchments hydrology but the requirement for them to be optimised

258

in order to fit the model may result in parameter estimates which bear no semblance to their true value in the field.

Many CRR models incorporate an optimisation algorithm which searches the n-dimensional parameter space for global optimum set of parameter values defined using some measure of model efficiency. For the purposes of model calibration HYSIM employs the Rosenbrock algorithm in conjunction with a number of objective functions. While in theory an optimum parameter set may exist, finding this point presents difficulties given the complexities of the response surface as well as the limitations of search algorithms and the differing efficiency criteria of objective functions. Sorooshian and Gupta (1995) highlight a number of difficulties associated with the parameter response surface which are common to CRR models. These include the presence of several major regions of attraction into which the search algorithm may converge and the existence of multiple local optima on the response surface. Furthermore where parameters exhibit varying degrees of sensitivity a great deal of interaction and compensation may be evident. The problems associated with determining a global optimum parameter set gives rise to uncertainties in model simulations.

The idea that one optimum model or parameter set exists has been challenged by the concept of 'equifinality' (Beven, 2007); that multiple parameter sets can be found, perhaps in very different regions of the response surface, all of which provide equally good performance scores (Duan et al., 1992; Freer et al., 1996). The concept also applies to different model structures. Essentially the theory suggests that there may be many representations of a catchment, consisting of numerous combinations of model structures and parameter values, which are equally valid in terms of their ability to provide acceptable simulations of the observed streamflow series. Conversely it has been shown that different parameter sets, all of which give comparable results during calibration, may yield significantly different results under forcing conditions on which the model has not been trained (Harlin and Kung, 1992). This demonstrates the uncertainty associated with model projections which arise from parameter uncertainty.

5.6.3 Artificial Neural Networks

This empirical approach to rainfall-runoff modelling is based solely on the inputs (precipitation and past discharge measurements) and outputs (current or future discharge) of a catchment system without any consideration given to the physical properties of the catchment itself. Essentially the catchment is treated as a 'black box' system, without any explicit consideration given to the internal processes and storage components which control how streamflow is

generated from rainfall. Despite omitting any representation of the internal physics of the catchment system, the ability of ANNs to model complex and highly dynamic non-linear systems mean they have gained popularity in the field of hydrological modelling. Given the responsive nature of each study catchment, underlined by the high correlation shown between daily rainfall and streamflow records, neural networks were thought to provide an adequate means of modelling the rainfall-runoff relationship.

The collective behaviour of an ANN, like the biological neural system on which it is based, demonstrates the ability to learn, recall and generalise from training patterns and experienced data. Neural networks are organised as layers of parallel processing nodes called neurons which are the basic elements of the network and make up its underlying structure. The set of neurons in each layer are connected via a series of weighting functions to all the neurons in the proceeding layer. The action of each neuron is to calculate a response based on the weighted sum of its inputs using a predetermined activation function. In order to learn the relationship between the input and target variables the network must undergo a training process. During this the connection weights are iteratively adjusted until the predicted network output best matches the observed system output. At this point the network is said to have learned the relationship between the input and output training datasets. The exact nature of the relationship cannot be extracted from the neural network but is rather contained in the optimised weighting values and connections between nodes. In this context ANNs can be considered as the 'ultimate black box model' (Minns and Hall, 1996). Two types of neural networks, a feedforward (static) network and a dynamic network, were assessed to determine their suitability for this study. The former is determined solely by the input-output pattern and has no feedback elements or time delays. Conversely using dynamic networks the model output depends not only on the current input but also on the previous inputs, outputs, or states of the network. Using dynamic networks allows information on antecedent conditions in the catchment, relating to both precipitation and flow levels, to be incorporated in the model. This is an important consideration given the significant influence preceding conditions can have on high flow and flooding events.

5.6.4   Training and Validating Models

HYSIM training and validation

Parameters within HYSIM can be divided into two categories; the physically based parameters and process or free parameters. The physical parameters for each study catchment were derived using GIS (Geographical Information System) mapping software. The use of GIS ensures that the information required by the model is objectively defined and grounded in

physically reality - thereby reducing the uncertainty associated with parameter estimates. The first task was the delineation of each catchment boundary using the Environmental Protections Agency's (EPA) Digital Elevation Model (DEM) (Smith, 2005). Digital terrain analysis tools specifically for the purposes of deriving watershed characteristics are available to supplement basic GIS tools and were employed in this study. Soil hydrological properties for each catchment were derived from the General Soil Map of Ireland (Gardiner and Radford, 1980). The soil association for each catchment was subsequently determined using information from the soils map. The dominant soil texture was calculated by establishing the percentage sand, silt and clay in each soil association with the derived texture being used to calculate the models soil parameters. So that the hydrological significance of different soils was given proper consideration in the model the proportions of each soil as well as its location within the catchment were taken into account when setting the parameter values. Vegetation parameters were obtained using the CORINE land-cover (Coordination of Information on the Environment) dataset (O'Sullivan, 1994). Owing to the lumped nature of the model the land-use type shown to be dominant in each catchment were used to define the land-use parameters. Finally the groundwater parameters were derived using an analysis of flow records and an examination of the underlying groundwater properties for each catchment taken from the Aquifer Map of Ireland (GSI, 2003).

In contrast, the process parameters are derived by minimising the difference between observed and simulated flows using a local search technique. To address parameter uncertainty and to negate the problems associated with determining a single optimum parameter set, the Generalised Likelihood Uncertainty Estimation (GLUE) procedure, a methodology based on the equifinality of parameter sets, was implemented in this study (Beven and Binley, 1992). GLUE is a well established method for uncertainty analysis and has been widely applied in the field of hydrological modelling (e.g. Beven and Binley, 1992; Beven, 1993; Freer, 1999; Cameron et al., 1999; Blazkova and Beven, 2002; Montanari, 2005, 2007).

The underlying principle of the GLUE procedure is that many 'behavioural' parameter sets exist and consequently it is only possible to assign a likelihood value to each one indicating whether it can adequately replicate the system and provide an acceptable or behavioural simulation of the observed flow (Beven and Binley, 1992). This method facilitates the assessment of parameter uncertainty by allowing probability bounds or confidence limits to be constructed based on the distribution of the combined model projections derived from each plausible parameter set. This approach to model calibration also has the advantage of allowing

the interaction between parameters to be implicitly accounted for as whole parameter sets are varied rather than varying individual parameters.

The GLUE procedure has the five main steps (Beven and Binley, 1992):

1. The definition of a likelihood measure, chosen on the basis of an objective function to determine model performance
2. The definition of a prior distribution for each parameter
3. Parameter sets are sampled from the defined prior distributions using sampling techniques such as Monte Carlo Random Sampling and Latin Hypercube Sampling
4. Each parameter set is classified as behavioural or non-behavioural through assessing whether it performs above or below a specified threshold
5. Predictive model runs generate results from each of the parameter sets that yield acceptable calibration simulations. These combined simulations are in turn used to determine the weighted mean discharge and simulation probability bounds (Melching, 1995)

For this study the GLUE procedure was employed as part of the modelling strategy for each catchment. Before the procedure was implemented a sensitivity analysis was firstly undertaken. Essentially this type of analysis is used to determine the sensitivity of the model output to changes in a given parameter. The results from this highlighted those parameters which had the greatest influence on the model response and as such warranted inclusion in the GLUE procedure. By drawing attention to those parameters which are poorly identified in the model structure the sensitivity analysis allows for a more efficient and effective calibration process.

For the purposes of this study a regional sensitivity analysis (RSA) was employed (e.g. Hornberger and Spear, 1981; Young, 1983; Beck, 1987). This method provides a measure of the absolute sensitivity of the model parameters and gives some indication of the level of interaction between them. The technique employs a Monte Carlo simulation procedure to run the model with randomly generated parameter sets. Visual inspection of the resulting 2-D dotty plots was used to determine the most sensitive parameters. Those which were well defined in the model structure produced the best efficiency scores within a narrow parameter range, for those which were relatively insensitive good simulations were produced using values sampled right across the parameter space. Based on the results of the sensitivity analysis the models four process parameters, as well as the parameters representing groundwater recession and the pore size distribution index, were selected for inclusion in the GLUE

procedure. Table 5.7 lists the parameters selected and their initial ranges for Monte Carlo sampling.

Table 5.7 HYSIM parameters included in GLUE analysis and initial parameter bounds sampled

Parameter	Minimum Value	Maximum Value
Saturated Permeability at the Horizon Boundary	1	250
Saturated Permeability at the Base of the Lower Horizon	1	250
Interflow Run-off from the Upper Horizon at Saturation	1	250
Interflow Run-off from the Lower Horizon at Saturation	1	250
Groundwater Recession	0.05	0.99
Pore Size Distribution Index (PSDI)	500	6000

The likelihood measure adopted for all catchments was the Nash Sutcliffe efficiency criterion:

$$1 - \frac{\sum (R_i - S_i)^2}{\sum (R_i - \bar{R}_i)^2}$$

Equation 5.1

where,

R represents recorded streamflow,

S is simulated streamflow, and

$\bar{R}$ is the mean of the recorded flows.

Based on this, parameter sets which attained a score above 0.7 over the calibration and validation period were considered to be behavioural. For the purposes of generating random parameter sets, the ranges used to delineate the sampling space had to be specified. This process was informed using a sensitivity analysis and empirical testing of possible parameter bounds. Care was taken to ensure that an adequate region of the parameter space was considered where behavioural sets were shown to exist. Using a Monte Carlo random sampling strategy 10,000 parameters sets were generated from a uniform distribution within the given ranges for each parameter. HYSIM was run using each randomly generated parameter set over the calibration period. Due to the differing lengths of observed precipitation and streamflow data which were available different calibration and validation periods were selected for each catchment (Table 5.8). All those parameters which met the required efficiency score over the calibration period were retained. In order to validate these parameter sets a blind simulation was conducted on each set for the validation period. The 20 best performing behavioural parameter sets over this period were considered to provide equally plausible representations of the catchment and used in the climate impact analysis presented in the following sections.

Table 5.8 Calibration and validation periods for each catchment and the max and min efficiency scores obtained

Catchment	Calibration	Max	Mean	Validation	Max	Mean
Altahoney	10/2002 - 6/2007	0.74	0.73	07/2007 - 07/2009	0.75	0.73
Goulan	10/2002 - 5/2007	0.76	0.72	06/2005 - 05/2006	0.76	0.72
Srahrevagh	10/2002 - 7/2007	0.75	0.72	09/2007 - 08/2009	0.71	0.70
Glendahurk	06/2003 - 3/2007	0.72	0.71	04/2007 - 07/2009	0.72	0.72
Glenamong	07/2002 - 3/2007	0.84	0.78	04/2007 - 04/2009	0.78	0.71
Maumaratta	07/2002 - 3/2007	0.66	0.64	04/2007 - 04/2009	0.65	0.62

ANN Training and Validation

In the present study a two-layer feed-forward network, comprised of a hidden layer with ten nodes and an output layer with single node, was used to predict catchment discharge on a daily time step taking precipitation and PE as the model inputs. The tan-sigmoid function was used as the hidden nodes activation function whilst a linear function was applied to the output node. A trial and error method was used to select the optimum number of hidden nodes. The network was trained over the calibration period (Table 5.8) using the scaled conjugate gradient backpropagation algorithm.

The use of dynamic networks is an attempt to capture the dynamic nature of the hydrological system and has the advantage of allowing 'memory' to be built into the model. To determine an optimum model structure a number of different dynamic networks were tested. This included networks with various time delays on their input and feedback connections. The use of delayed inputs allows rainfall at both current and previous time intervals to be considered as contributors to catchment discharge. Preliminary work by Hall and Minn (1993) indicated that the number of antecedent rainfall ordinates required was broadly related to the lag time of the drainage area, reflecting the time differential in the routing of precipitation from different areas of the catchment to its outlet point. Incorporating a feedback mechanism (i.e. the use of an output variable as a model input) in the model structure allows river levels from the preceding days to be considered when determining catchment discharge on a given day. Past studies have used runoff from previous time steps as one of the inputs to the model in order to represent conditions in the catchment (e.g. soil moisture). This may be important given the role catchment conditions play in determining runoff behaviour. The common underlying structure used for each dynamic network, including the number of layers and activation functions used, followed that outlined for the feed-forward network. In addition the same training algorithm was used.

Table 5.9 outlines the various dynamic network configurations considered. Also listed is the percent explained variance (R^2) for each model, including the feed-forward network and CRR model, for the calibration and validation periods. Int represents model input (precipitation and PE) at time t and Qt represents catchment discharge at time t.

Table 5.9 Comparison of performance of each modelling approach for the calibration and validation period in the Glenamong catchment. Model performance is evaluated using percent explained variance (R^2)

Modelling Approach	Calibration (E %)	Validation (E %)
HYSIM	85	81
Feed-Forward (Int)	76	71
Dynamic Network Configuration		
Int and Int-1	82	80
Int, Int-1 and Int-2	82	80
Int, Int-1 and Qt-1	86	82
Int, Int-1, Qt-1, Qt-2 and Qt-3	85	81
Int, Int-1, Int-2, Qt-1 and Qt-2	88	83

Both the dynamic neural networks and CRR model were shown to account for a higher proportion of the variance exhibited in the observed series when compared to the feedforward network. This model was also shown to vastly underestimate high flow events. The performance of each model suggests that the use of rainfall inputs alone is insufficient and that those networks which included some feedback or input delay mechanisms provided a better representation of the system. This is in-line with findings from previous studies (Minns and Hall, 1996; Campolo et al., 1999; Rajurkar, 2004).

There was little variation in the performance of different dynamic network configurations. However increasingly complex model structures, which considered greater time lags, did perform worse than those models which took account of antecedent rainfall and flow ordinates from two to three days pervious. This indicates that the catchment has a short memory i.e. the influence of a rainfall event on the catchments hydrology lasts only for a day or two. The comparable performance of HYSIM and the neural networks suggests that an empirical approach was adequate for modelling the relationship between rainfall and catchment runoff. To assess model uncertainty, HYSIM and the final dynamic neural network listed in Table 5.9 were both used to simulate streamflow using the same climate scenario. Both models produced very similar results under future climate forcing.
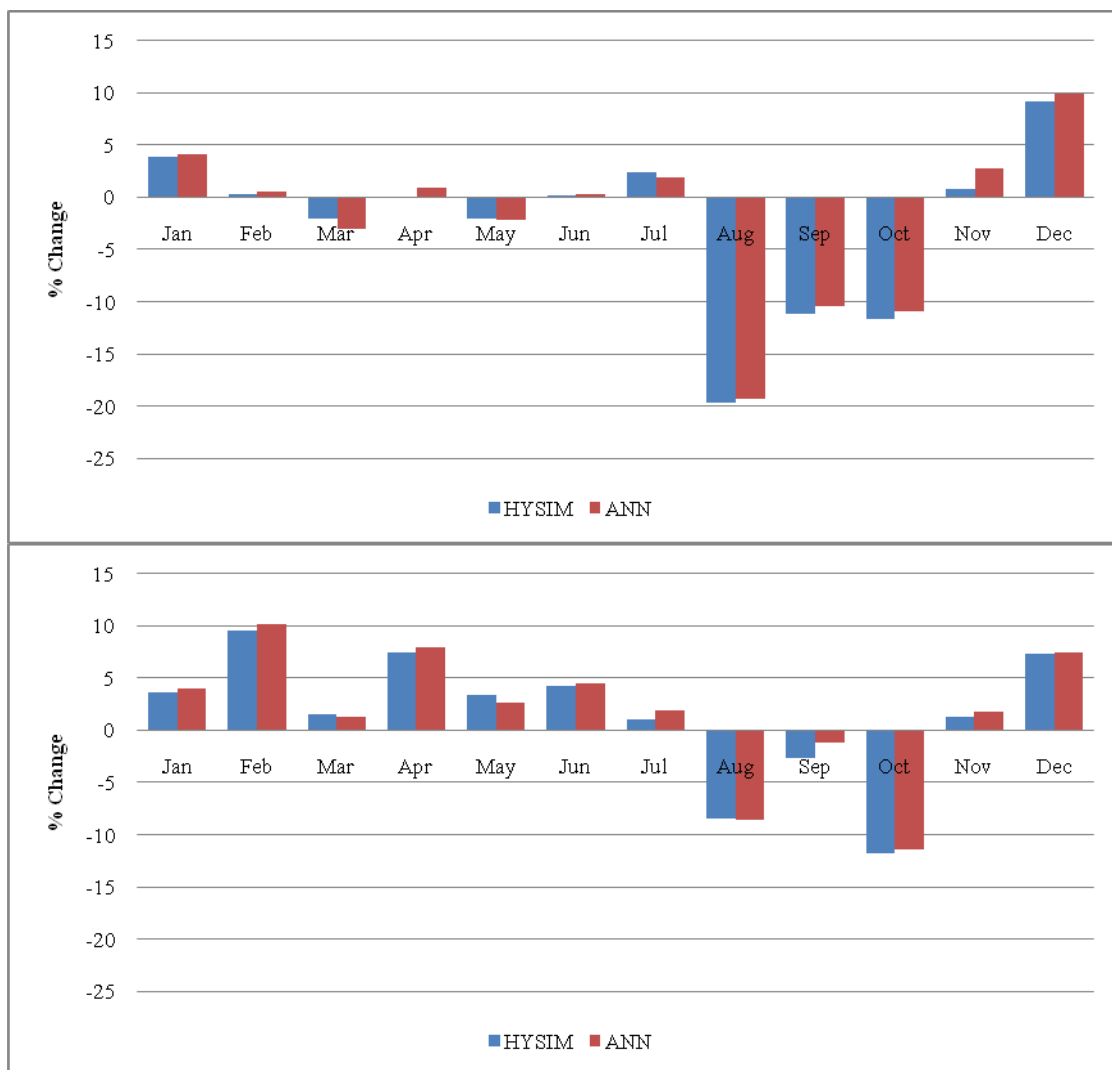
Figure 5.4 Percentage change (%) in mean monthly streamflow for the Glenamong catchment simulated using HYSIM and ANN for the 2050s (top) and 2080s (bottom). Both models are run using data from the HadCM3 GCM under the B2 emissions scenario.

Figure 5.4 illustrates the monthly percent change in mean streamflow, as simulated by the selected neural network and HYSIM, using climate projections downscaled from the HadCM3 GCM. Given the agreement shown between each models simulated changes in the Glenamong flow regime it was assumed that the uncertainty associated with the final streamflow projections arising due to model choice would be negligible. Consequently only HYSIM was employed to model future streamflow for the remaining catchments. This model was selected over the ANNs as it allows for the hydrological dynamics of the catchment to be explicitly represented in the model structure.

5.7   Extreme Value Analysis

In order to examine changes in frequency of flooding in each of the catchments modelled, an extreme value analysis was conducted to assess how the frequency of selected flood events for the control period are likely to change for each future time period. In total six flood events

were chosen; the flood expected every 2, 5 10, 15, 20 and 50 years. Therefore flood events ranging from fairly frequent (2-year) to moderately infrequent (50-year) are analysed. Due to the limited years of data more extreme return periods were not included. One of the key assumptions of flood frequency analysis is that the return period of a flood peak of a given magnitude is stationary with time (Cameron et al., 2000). However, a number of studies (Arnell and Reynard, 1996; Hulme and Jenkins, 1998) have demonstrated the variability of climate characteristics, with such variability having implications for statistical methods used in flood frequency analysis. Consequently assumptions regarding the stationarity of the flood series are made. In dealing with non-stationarity in the flood series Prudhomme et al. (2003) contend that it is possible to assume stationarity around the time period of interest (i.e. the thirty year periods represented by the 2020s, the 2050s and 2080s). Under this assumption, standard probability methodologies remain valid and are thus considered representative of the flood regime of the time horizon considered (Prudhomme et al., 2003). Similar assumptions are made in this work.

For each realisation of future streamflow the maximum annual flood series was extracted for each future time period. Therefore, in each of the catchments a 30 year maximum annual flood (MAF) series was extracted for each simulation for the control period (1961-1990), 2020s, 2050s and 2080s. Having extracted the flood series an extreme value distribution was fitted to each series using the methods described in the Flood Estimation Handbook (FEH) (Robson and Reed, 1999).

The distribution employed for the analysis was the Generalised Logistic (GL) distribution, a three parameter distribution defined by:

$$Q(F) = \xi + \frac{\alpha}{\kappa}\left[1 - \left(\frac{1-F}{F}\right)^{\kappa}\right]$$ **Equation 5.2**

where,

ξ is the location parameter,
α is the scale parameter,
κ is the shape parameter, and
F is the non-exceedance probability.

The range of possible values for the GL distribution is:

$$-\infty < Q \leq \xi + \frac{\alpha}{\kappa} \qquad \text{if } \kappa > 0$$

$$\xi + \frac{\alpha}{\kappa} \leq Q < \infty \qquad \text{if } \kappa < 0$$

267

Therefore the GL distribution is bounded above for $\kappa > 0$ and bounded below for $\kappa < 0$ (Robson and Reed, 1999). Using the FEH methodology, the GL growth curve is obtained by substituting $x = Q/\xi$ into the equation for the GL distribution and rearranging to give:

$$x(F) = 1 + \frac{\beta}{\kappa}\left[1 - \left(\frac{1-F}{F}\right)^{\kappa}\right]$$ **Equation 5.3**

where

$$\beta = \alpha / \xi$$

(Robson and Reed, 1999)

The growth curve can also be written in terms of the return period T:

$$x_T = 1 + \frac{\beta}{\kappa}\left[1 - (T-1)^{-\kappa}\right]$$ **Equation 5.4**

The growth curve is also bounded above for $\kappa > 0$. The parameters of the GL growth curve are calculated by fitting the distribution to observed data. There are a number of different techniques that can be used for this purpose, including the method of moments, Maximum Likelihood Estimation and the L-moment approach. In this work the latter is employed to fit the GL distribution to the MAF series of each simulation. Hosking and Wallis (1997) highlight some of the benefits of the method of L-moments over alternative methods of distribution fitting. For example, L-moments are more suited to flood analysis than ordinary moments due to the skewness of the flood series, while the method of L-moments has been shown to be more reliable than maximum likelihood estimation in situations were only small or medium sized samples are available, as is the case here with 30 years of data in each MAF series. In order to fit a distribution to a flood series, sample L-moments are calculated from the flood data using unbiased probability weighted moment estimators (Landwehr et al., 1979).

The frequency of flows associated with each return period during the control period was assessed for each future time period. Robson and Reed (1999) highlight that for the GL distribution the return period for a flow of a certain magnitude is given by:

$$T = 1 + \left[1 - \frac{\kappa}{\alpha}(Q - \xi)\right]^{\frac{-1}{\kappa}}$$ **Equation 5.5**

Therefore in each catchment for each future time period new return periods are derived for the flow attributed to the 2, 5, 10, 15, 20 and 50 year floods under the control period. Results for each catchment are detailed below.

5.8   Future Hydrological Impacts of Climate Change

Future streamflow for each of the six catchments selected was modelled using meteorological data for the period 1961-2099 downscaled from three GCMs (HadCM3, CSIROmk2 and CGCM2) each run using two different emission scenarios (A2 and B2). Employing multiple GCMs, emission scenarios and downscaling methods allows the uncertainties associated with local scale estimates of climate change to be accounted for in streamflow projections. The incorporation of the stochastic element in SDSM downscaling allows an element of natural variability to be included in future simulations. HYSIM was employed to simulate catchment discharge on a daily time step using precipitation and potential evaporation as model input.

For future runs the hydrological model is used with parameter sets fitted on observed data, with the assumption that catchment parameter sets are not dependent on climate, i.e. that the processes involved in the physical transformation of precipitation into streamflow are independent from climate. The majority of climate change impact assessments are based on this assumption (Booij, 2005; Wilby, 2005; Fowler and Kilsby, 2007; Prudhomme and Davies, 2009). Giving weight to this assumption, Neil et al. (2003) highlight that there is no evidence that non-stationarity in climate would incur parameter instability. In order to account for parameter uncertainty 20 parameter sets, each of which were shown to provide an equally plausible model of the catchment system under observed conditions, were employed when simulating streamflow under the forcing conditions of future climate scenarios. Thus, in total over 12,000 simulations were produced for each catchment, sampling across the uncertainty range in employed GCMs, emission scenarios, downscaling technique and hydrological model uncertainty.

Projected changes in streamflow for each study catchment are considered for three future time horizons the 2020s (2010-2039), 2050s (2040-2069) and 2080s (2070-2099), with the period 1961-1990 used to represent baseline or reference conditions. For each catchment changes in the monthly flow regime and for high and low flow events were considered. Changes in the monthly flow regime for each catchment are presented using box plots. The whiskers represent the 95% confidence intervals of projected changes, also presented are the 75th and 25th percentiles and the mean (middle line). Changes in the monthly flow regime are presented relative to the natural variability for the current climate.

5.9   Uncertainty in Future Hydrological Simulations

As a first component of the analysis a comparison of the sources of uncertainty considered was carried out for the Glenamong catchment. By far the largest component of uncertainty is derived from the use of different GCMs. Figure 5.5 shows the changes in the monthly flow regime for the Glenamong catchment for each of the GCMs considered, all other sources of uncertainty were held constant (i.e. one emissions scenario (A2), one downscaling technique (SDSM) and one parameter set). Evident is the fact that there is a good deal of deviation in relative changes between climate models in relation to both the timing and magnitude of changes in the monthly flow regime. Of particular note are the large reductions in spring flow simulated by CGCM2 climate model, particularly by the 2080s. The HadCM3 model tends to be the driest model with the largest decreases in flow associated with the 2080s. The disparities between models emphasise the importance of including multiple GCMs in impact assessment in order to increase the robustness to uncertainty of policy making in adapting to climate change.

In relation to the uncertainty in future flows derived from greenhouse gas emissions, Figure 5.6 depicts the results for the Glenamong catchment. In assessing the contribution from this source of uncertainty only the emissions scenario was varied between both sets of simulations. Obvious from the results is that the A2 scenario simulates greater increases in winter flows and greater reductions for summer and autumn flows than the more optimistic B2 emissions scenario. Divergence between the scenarios is greatest after the middle of the century and largest by the 2080s. For the B2 scenario no changes in the flow regime are significant outside of natural variability, even by the 2080s. While the uncertainty between emissions scenario is important, it is not as large as the uncertainty derived from the use of different GCMs.

A final source of uncertainty analysed here is that derived from parametric sources in the HYSIM model due to issues non-identifiability of an optimum parameter set. Within this experiment only the behavioural parameter sets were varied. Of interest is the range of changes characterised by the box plots (Figure 5.7). For the winter months the range of uncertainty is small with greatest uncertainties evident for spring and summer months. There is also an increase in uncertainty from the 2020s to the 2080s. However, in comparison to GCM uncertainty, parameter uncertainty from HYSIM is small, but can be as large as emissions scenario uncertainty during summer months. This is consistent with the findings of Wilby and Harris (2006).
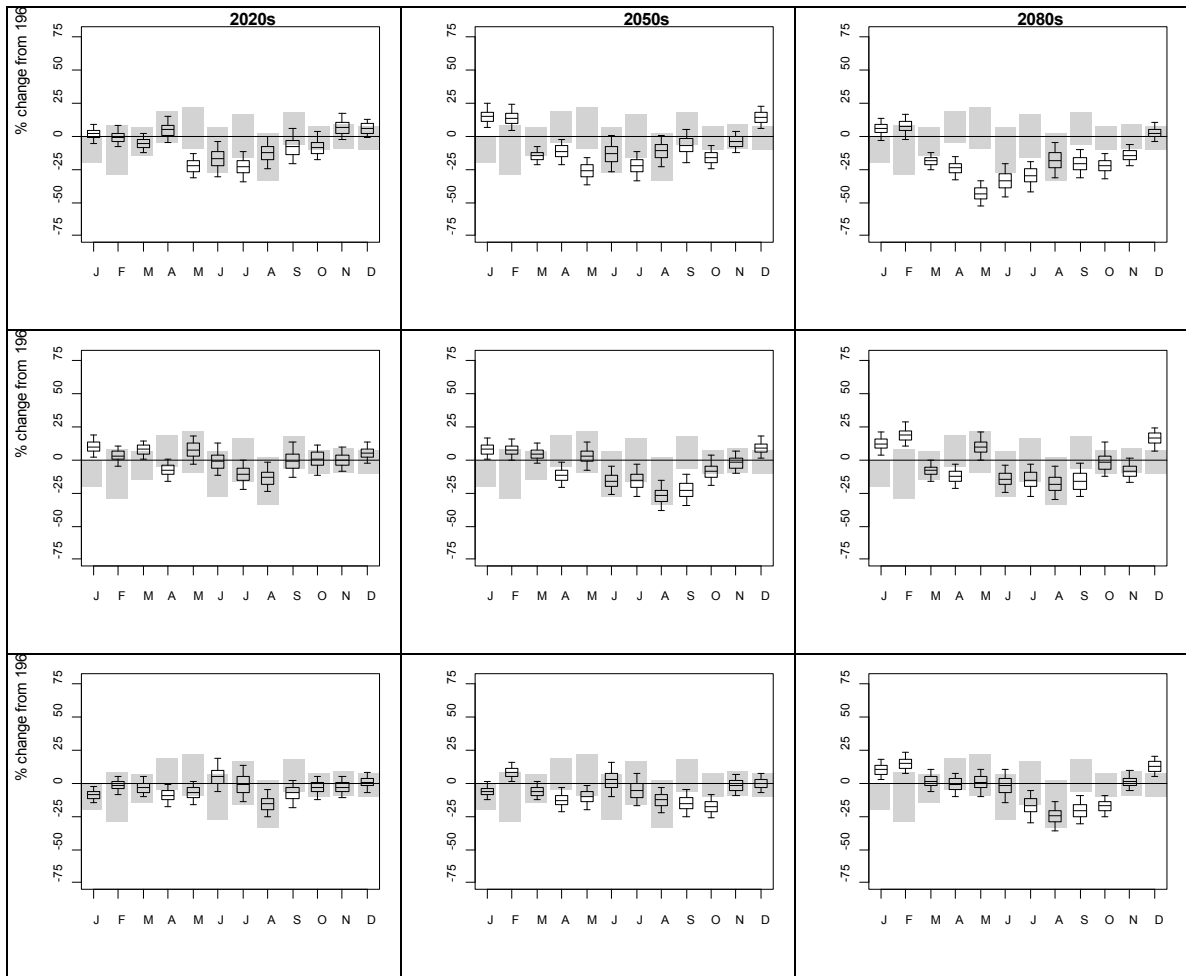
Figure 5.5 Uncertainty in changes in future flow regime derived from GCMs CGCM2 (top), CSIRO-Mk2 (middle) and HadCM3 (bottom).
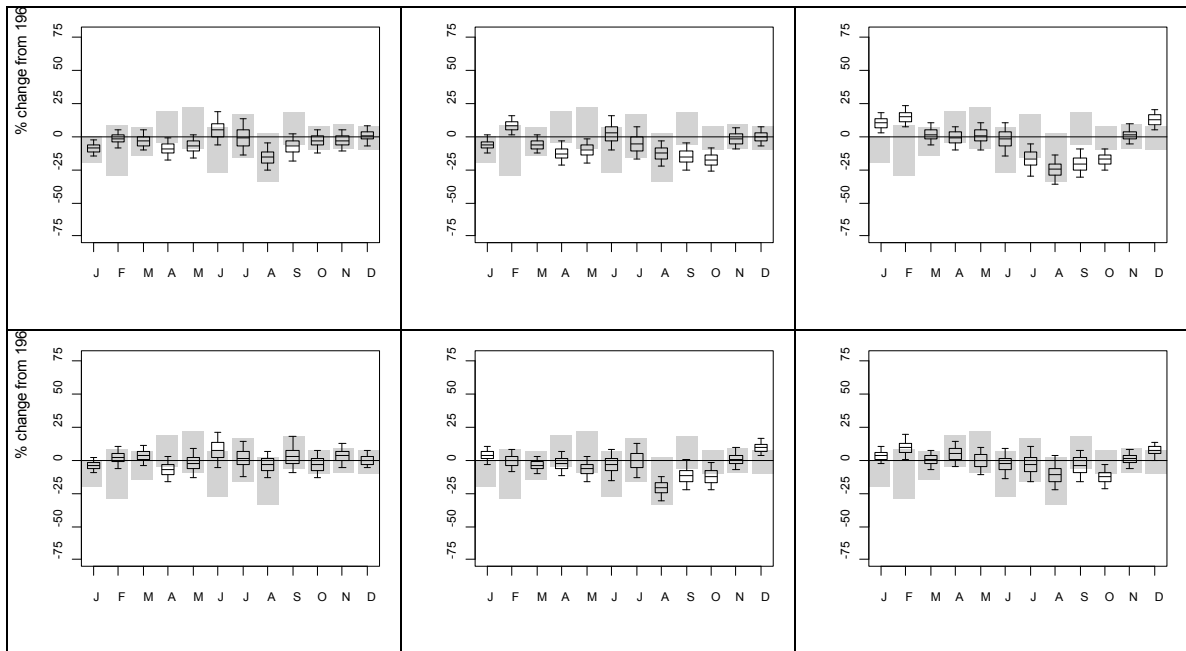

Figure 5.6 Uncertainty in changes in future flow regime derived from emissions scenarios. Both A2 (top) and B2 (bottom) are run using HadCM3.
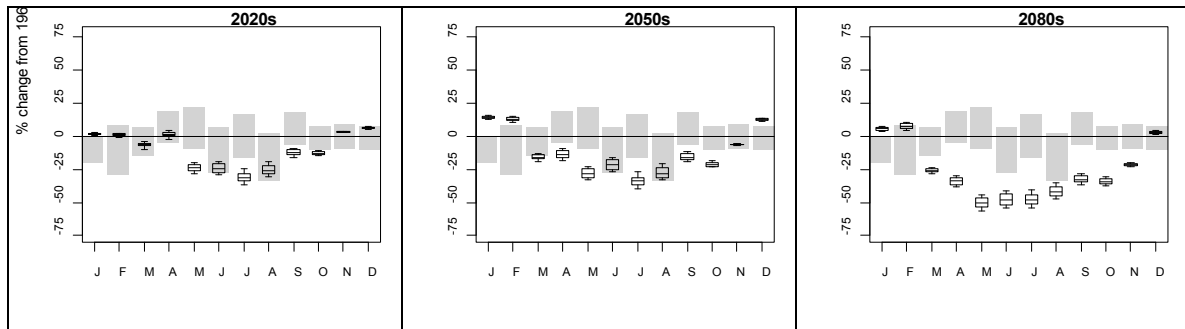
271

Figure 5.7 Uncertainty in changes in future flow regime derived HYSIM model parameters

5.10 Simulated Changes in Hydrology

5.10.1 Glendahurk Catchment

Changes in the monthly flow regime for the Glendahurk catchment are outlined in Figure 5.8. Evident is that fact that no clear signal of change is evident for the 2020s with results for each month spanning a sign change. Further, no changes are significant outside of natural variability for the control period. By the 2050s, while uncertainty ranges are still large there is clear evidence of a shift towards increased seasonality of flows with wetter winter and drier summers. Changes for May are significant outside natural variability, while the majority of runs show decreases in monthly flows from March through to October. By the 2080s the increased seasonality is further developed with significant increases in flow simulated for December and January of up to 25%, while significant decreases are suggested for June and October. For the remaining months the climate change signal is not deemed to be significant outside of natural variability.
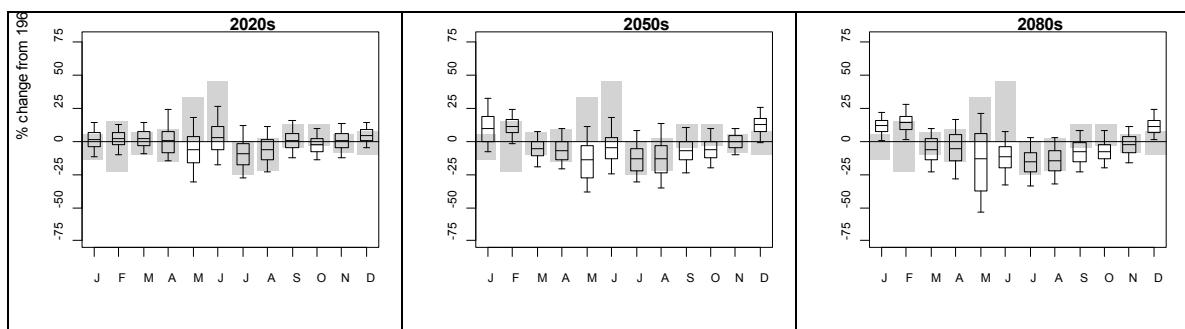

Figure 5.8 Changes in the monthly flow regime for the Glendahurk catchment for the 2020s, 2050s and 2080s relative to the control period 1961-90.

Changes in the full range of flow conditions were assessed by analysing changes in the flow percentiles for each future time period relative to the control period 1961-1990. Of particular interest are changes at the extremes of the flow distribution; represented as Q05, the flow exceeded only five percent of the time and representative of high flow conditions and Q95, the flow exceeded 95% of the time and representative of low flow conditions. Overall an increase

in high flows is likely, particularly by the end of the century; while a decrease in low flows are suggested for the majority of model runs. Changes in the tails of the flow distribution for the Glendahurk are further investigated below in Figure 5.9.
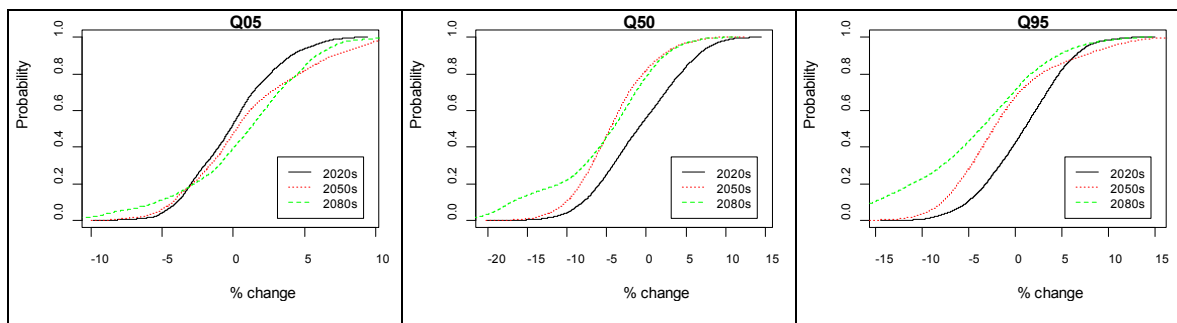

Figure 5.9 Cumulative distribution functions of percent changes in annual flow percentiles for the Glendahurk catchment.

Changes in the frequency of low flow events are presented in Figure 5.10. The flow threshold used to characterise low flow events is the Q95 for the relative season during the control period. To assess changes in the frequency, a count of the number of days in the year/season when flows fall below this threshold is conducted for each future time period. Results are presented as a change in the number of days relative to the control period 1961-1990. From the results obtained for the Glendahurk catchment an increase in the frequency of low flow events is suggested for each future time period with increases of 9.75, 11.2 and 30.12 days simulated for the 2020s, 2050s and 2080s respectively. Uncertainty ranges are large, particularly for the 2080s with changes ranging from a reduction of almost thirty days per year to an increase of up to 90 days a year. On a seasonal basis summer and autumn show the greatest increase in frequency of low flow days with uncertainty bounds again spanning a sign change. From all simulations a mean increase of approximately thirteen days is suggested for the summer by the end of the century.
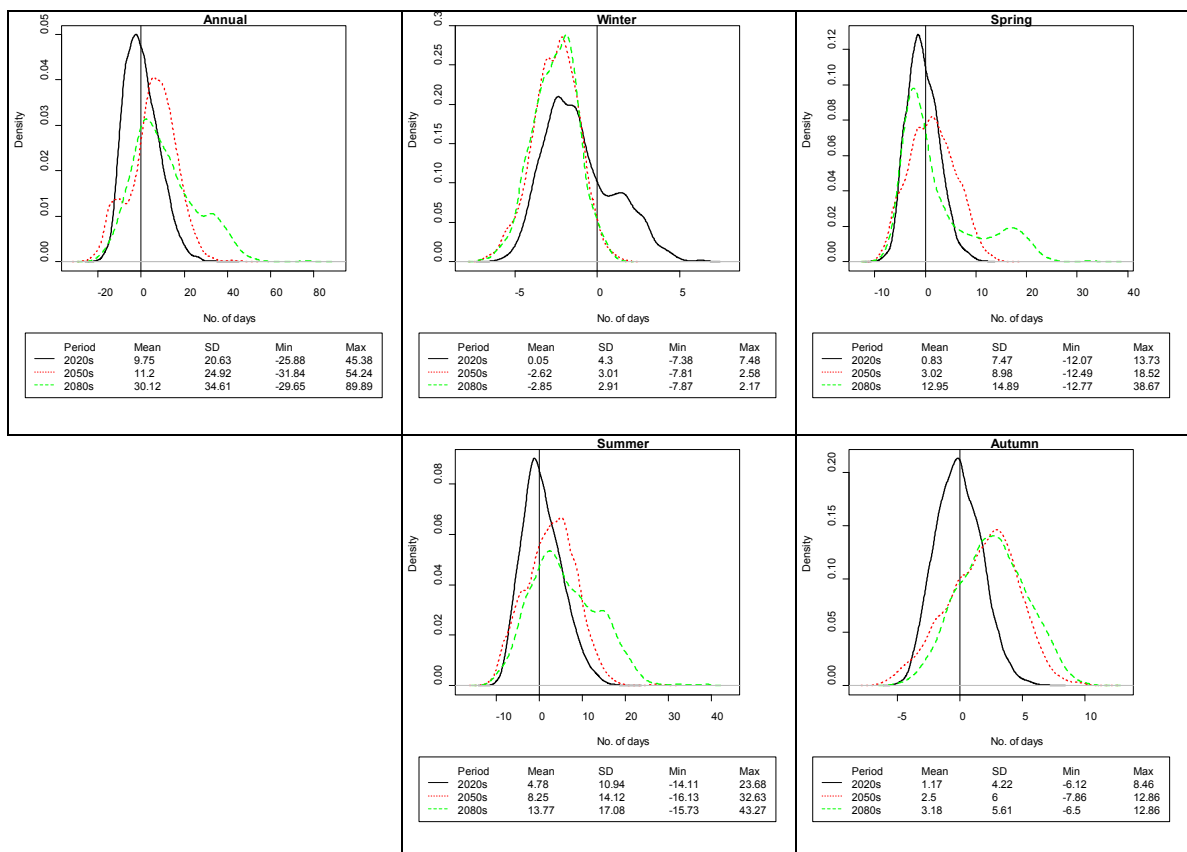
Figure 5.10 Simulated changes in the frequency of low flow events on an annual and seasonal basis for each future time period in the Glendahurk catchment

Figure 5.11 depicts the simulated changes in the duration of low flow events for the Glendahurk catchment. Calculation of the duration of low flow events was based on assessing the difference, for each future time period, in the cumulative number of days for which flows were below Q95 for the baseline period. On an annual basis a slight reduction in the duration of low flow events is evident for the 2020s, however for the end of the century an average increase in the duration of low flow events of approximately three days is suggested. The greatest increases in the duration of low flow conditions are shown for spring and summer, with the latter showing an increase of almost five days in the average duration of low flow conditions.
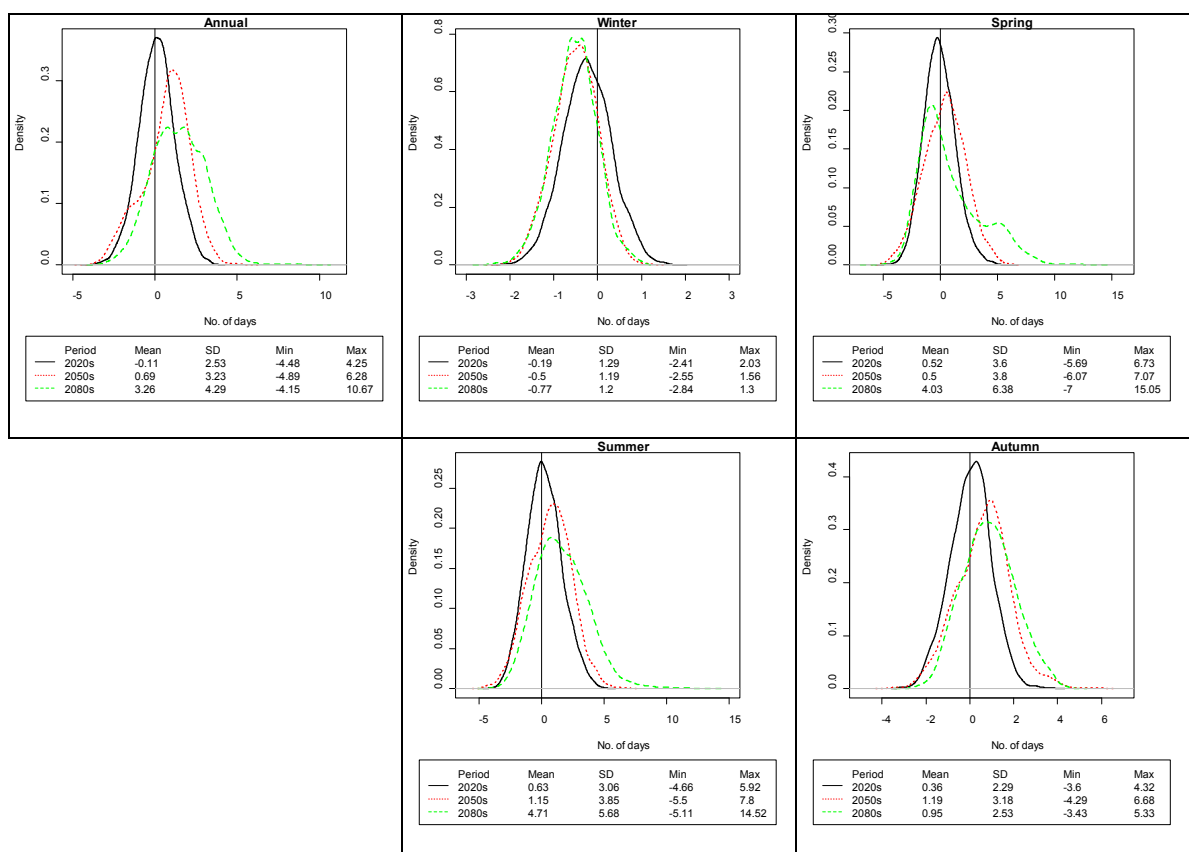
Figure 5.11 Simulated changes in the duration of low flow events on an annual and seasonal basis for each future time period in the Glendahurk catchment

In relation to the frequency of flood events Table 5.10 shows the changes in the frequency of selected flood events for each future time period. Particular emphasis is given to the uncertainty in future frequencies derived from each of the GCMs and emission scenarios employed. For each future time period the greatest increases in frequency are derived from the CGCM2 model which shows a consistent increase in frequency for all flood events for each time period. On the other hand a reduced frequency of occurrence of the selected flood events is suggest by the CSIRO A2 and B2 runs and Hadley A2 runs for the 2020s and 2050s. However, by the end of the century all runs with the exception of CSIRO B2 suggest and increase in the frequency of selected flood events. In the most extreme case (CGCM2 A2) the current flood with a return period of 50 years is likely to occur once every ~9 years.

Table 5.10 Changes in the frequency of selected flood recurrence intervals from the control period for each future time period for the Glendahurk catchment.

2020s	CGCM2-A2	CGCM2-B2	CSIRO-A2	CSIRO-B2	HADCM3-A2	HADCM3-B2
t2	1.95	2.87	1.69	2.405	1.05	1.78
t5	3.76	4.99	4.42	7.79	17.05	4.45
t10	6.1	7.02	10.05	17.35	73.26	9.02
t15	8.07	8.5	16.87	26.91	138.25	13.45
t20	9.7	9.61	24.19	36.82	204.59	18.04
t50	17.67	14.37	81.91	96.27	588.55	44.52
2050s	**CGCM2-A2**	**CGCM2-B2**	**CSIRO-A2**	**CSIRO-B2**	**HADCM3-A2**	**HADCM3-B2**
t2	1.65	2.74	2.01	1.53	2.02	2.17
t5	2.67	5.0	6.7	3.16	6.14	6.11
t10	3.95	6.02	15.23	5.85	15.2	12.97
t15	5.03	6.54	24.48	8.47	26.21	19.75
t20	5.92	6.85	33.51	11.15	38.78	26.86
t50	10.37	7.85	92.59	27.04	143.3	69.21
2080s	**CGCM2-A2**	**CGCM2-B2**	**CSIRO-A2**	**CSIRO-B2**	**HADCM3-A2**	**HADCM3-B2**
t2	2.37	2.4	1.53	1.79	1.39	1.59
t5	3.61	3.99	3.43	4.61	2.68	2.86
t10	4.79	5.47	7.49	10.03	4.54	4.17
t15	5.61	6.53	12.68	15.92	6.16	5.11
t20	6.23	7.31	18.43	22.42	7.62	5.91
t50	8.74	10.6	70.53	67.61	14.94	9.01

5.10.2   *Glenamong Catchment*

Projected changes in the mean monthly flow regime for the Glenamong catchment are depicted in Figure 5.12. For the 2020s there is no clear indication of any significant changes in monthly streamflow outside the bounds of natural variability for reference climate conditions. A similar picture is produced from model simulations for the 2050s. However the seasonality of the discharge regime does begin to become more pronounced with significant changes in streamflow being registered for the months of January and April. By the 2080s changes in local climate conditions, i.e. drier summers and wetter winters, become more apparent in the projected flow regime. Increases in January, February and December are deemed to be significant whilst decreases in catchment discharge are significant for September and October. For the remaining months model simulations are not considered to be significant outside natural variability.
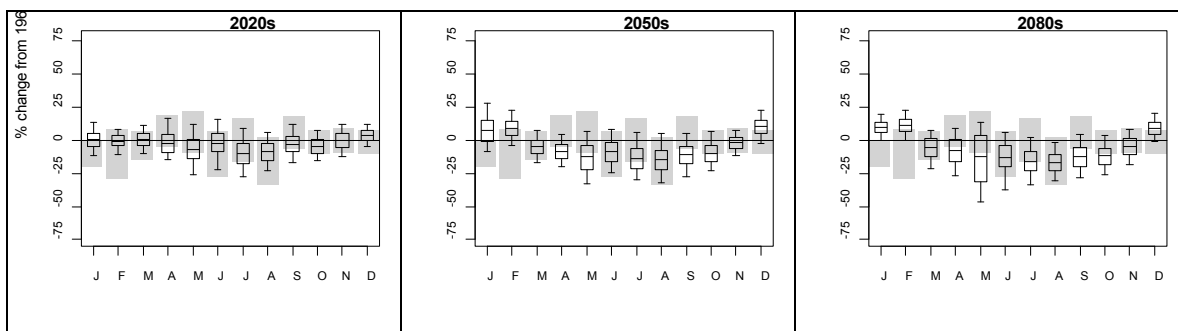
Figure 5.12 Changes in the monthly flow regime for the Glenamong catchment for the 2020s, 2050s and 2080s relative to the control period 1961-90

Model projected changes in the full range of flow conditions for the Glenamong catchment are assessed by examining changes in the annual flow percentiles for each future time horizon relative to the baseline period. Of particular interest are changes at the extremes of the flow distribution considered here using Q05 and Q95 flow percentiles. The cumulative distribution functions presented in Figure 5.13 depict the projected changes in each flow percentile. Model results suggest that an increase in high flows (Q05) is likely becoming more pronounced as the century progresses. A decrease in low flows (Q95) is also suggested, again with the trend becoming more acute towards the end of the century.
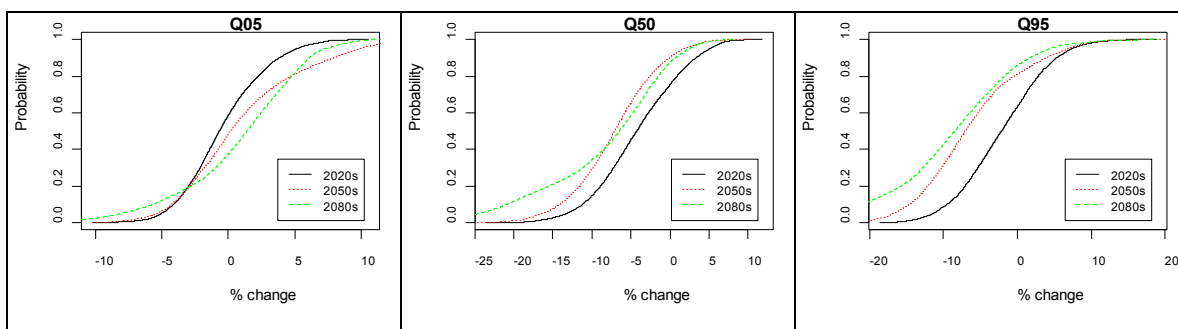

Figure 5.13 Cumulative distribution functions of percent changes in annual flow percentiles for the Glenamong catchment.

Changes in the frequency of low flow events are presented in Figure 5.14. From the results obtained for the Glenamong catchment an increase in the frequency of low flow events is suggested for each future time horizon - with increases of 15.2, 14 and 40.5 days projected for the 2020s, 2050s and 2080s accordingly. On a seasonal basis the greatest increase in the number of low flow days is projected to occur for the summer (18.27) over the 2080s horizon. Uncertainty ranges are also largest for this season, particularly for the 2080s, with model projections ranging from a reduction of almost sixteen days per annum to an increase of up to 52 days. The spring also exhibits a notable increase in low flow days for the same horizon (13.43) with uncertainty bounds again spanning a sign change (-14.63 to +41.5).
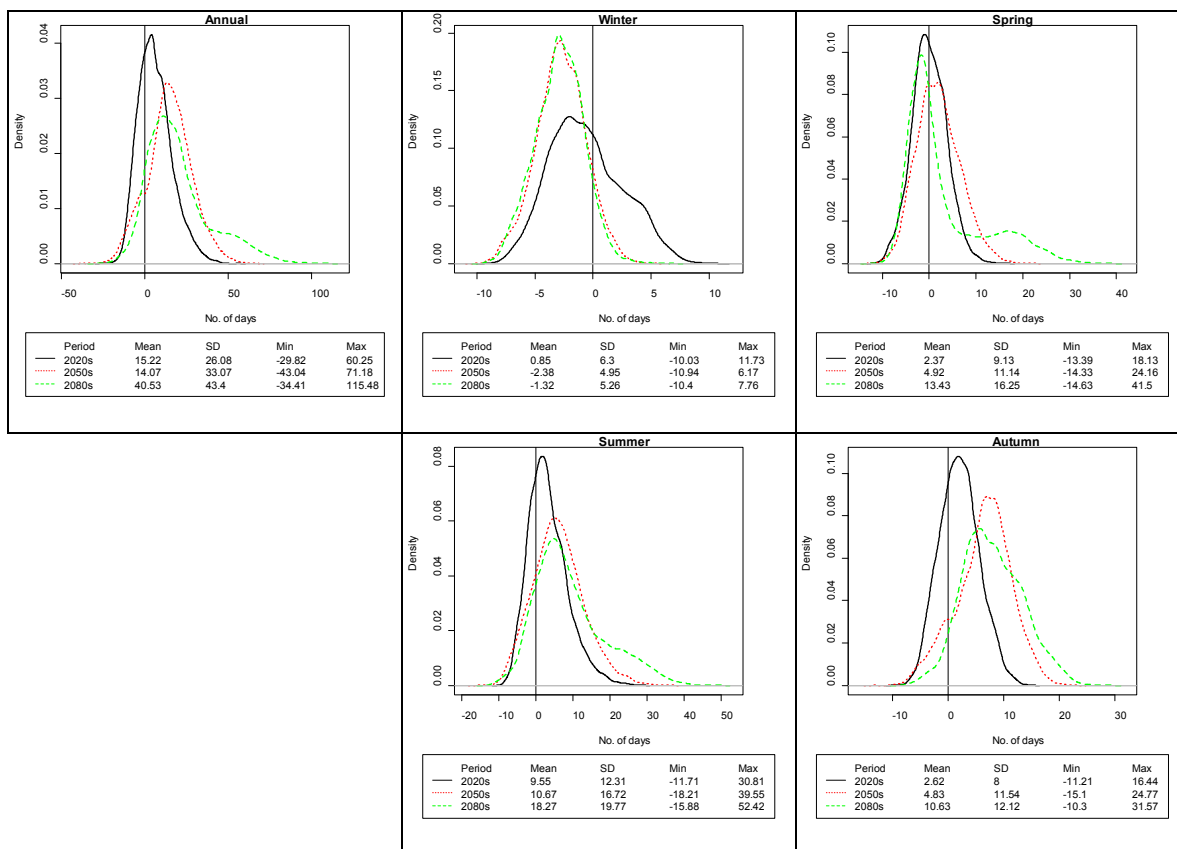
Figure 5.14 Simulated changes in the frequency of low flow events on an annual and seasonal basis for each future time period in the Glenamong catchment

Figure 5.15 displays the model projected changes in the duration of low flow events for the Glenamong catchment. On an annual basis an increase in the duration of low flow events is evident for each future time period with increases of 1.57, 2.26 and 2.89 days for the 2020s, 2050s and 2080s respectively. The greatest increases in the duration of low flow conditions are shown for spring and summer, with the latter showing an increase of over six days by the end of the century. The uncertainty bounds are also largest for these seasons with a standard deviation of 7.07 and 6 in the statistical distribution of model projections for the 2080s.
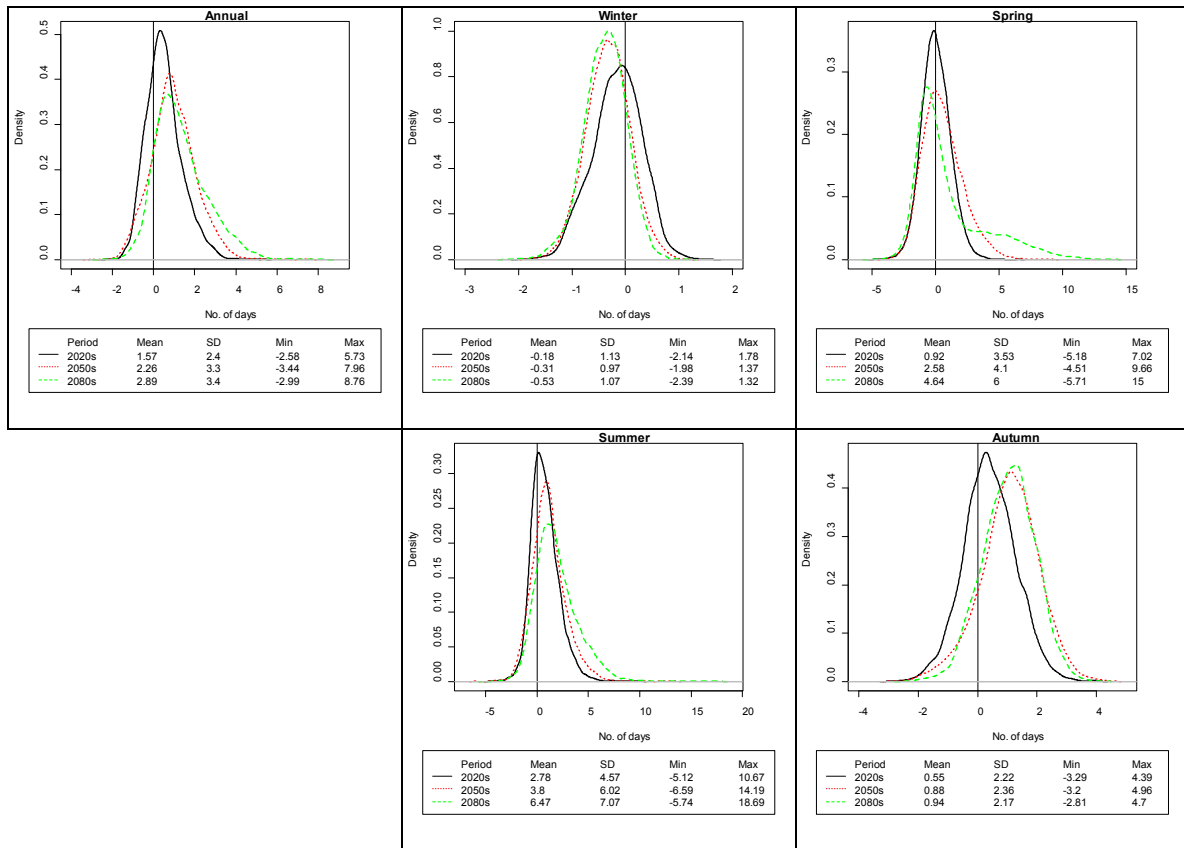
Figure 5.15 Simulated changes in the duration of low flow events on an annual and seasonal basis for each future time period in the Glenamong catchment.

Table 5.11 displays the model simulated changes in the return period for selected flood events. For each horizon the greatest increases in the frequency of flooding events are derived from the CGCM2 model, which exhibits a consistent decrease in the return period for each event over the three future horizons. Conversely a reduced frequency of occurrence for certain flooding events is suggested by the CSIROmk2 A2 and B2 model projections along with the HadCM3 A2. However by the end of the century all runs, with the exception of CSIRO B2, suggest a reduction in the return period of selected flood events. In the most extreme case (CGCM2 A2) it is suggested that the magnitude of a flooding event with a return period of 50 years under baseline conditions will occur once every 7.66 years by the end of the century.

Table 5.11 Changes in the frequency of selected flood recurrence intervals from the control period for each future time period for the Glenamong catchment

2020s	CGCM2-A2	CGCM2-B2	CSIRO-A2	CSIRO-B2	HADCM3-A2	HADCM3-B2
t2	1.89	2.81	1.67	2.31	1.72	1.71
t5	3.54	5.17	3.58	6.98	3.67	4
t10	5.51	7.56	6.77	15.21	6.7	7.83
t15	7.07	9.46	9.71	23.98	9.66	11.85
t20	8.46	11.06	12.67	32.87	12.79	15.78
t50	14.71	17.59	29.39	87.16	30.29	40.49
2050s	CGCM2-A2	CGCM2-B2	CSIRO-A2	CSIRO-B2	HADCM3-A2	HADCM3-B2
t2	1.6	2.08	2.03	1.43	2.13	1.64
t5	2.35	3.29	5.38	2.69	6.66	3.28
t10	3.14	4.46	11.26	4.89	15.25	5.64
t15	3.72	5.36	16.82	7.27	24.48	7.87
t20	4.21	6.11	22.52	9.73	34.93	9.91
t50	6.26	9.07	55.53	25.52	100.45	21.08
2080s	CGCM2-A2	CGCM2-B2	CSIRO-A2	CSIRO-B2	HADCM3-A2	HADCM3-B2
t2	2.32	2.27	1.45	1.7	1.39	1.58
t5	3.47	4.16	2.62	4.25	2.57	2.89
t10	4.47	5.98	4.62	8.98	4.25	4.32
t15	5.14	7.57	6.54	14.23	5.74	5.44
t20	5.67	8.93	8.53	19.71	7.2	6.35
t50	7.66	14.71	20.68	55.37	14.18	10.26

5.10.3 Maurmatta Catchment

Projected changes in the monthly flow regime for the Maurmatta catchment are outlined in Figure 5.16. No clear signal of change in monthly flows is exhibited for the 2020s with the majority of model runs for each month lying within the bounds of natural variability. Conversely by the 2050s there is clear evidence of a shift towards an increased seasonality in the flow regime. This finding is in-line with the anticipated occurrence of wetter winters and drier summers. Changes for the months of January, April and March are significant outside natural variability. The majority of model simulations exhibit decreases in monthly flows from March through to October. By the 2080s this increased seasonality is further amplified with significant increases in mean flow projected for the month of January, while significant decreases are suggested for June, August and September. The largest uncertainty bounds are associated with the month of May.
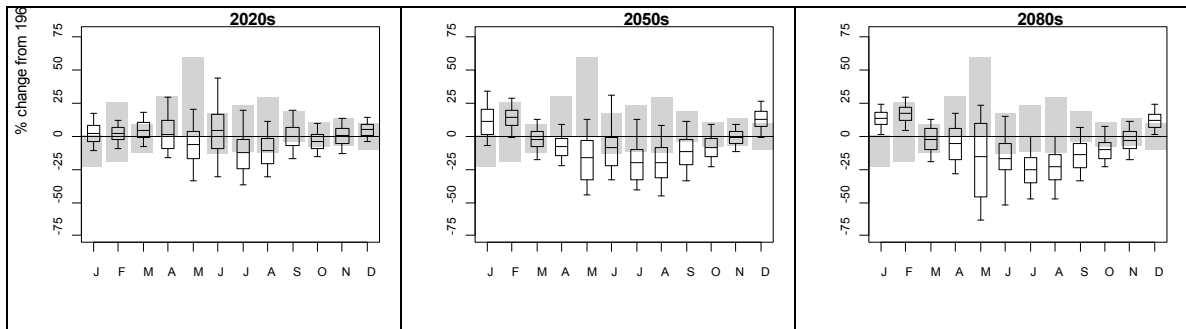
Figure 5.16 Changes in the monthly flow regime for the Maurmatta catchment for the 2020s, 2050s and 2080s relative to the control period 1961-90

From Figure 5.17 model simulations suggest that an increase in high flows is likely whilst a decrease in low flows is suggested for the majority of model runs. This underlying trend, of increases and decreases for Q05 and Q95 respectively, is anticipated to become more pronounced as the century progresses.
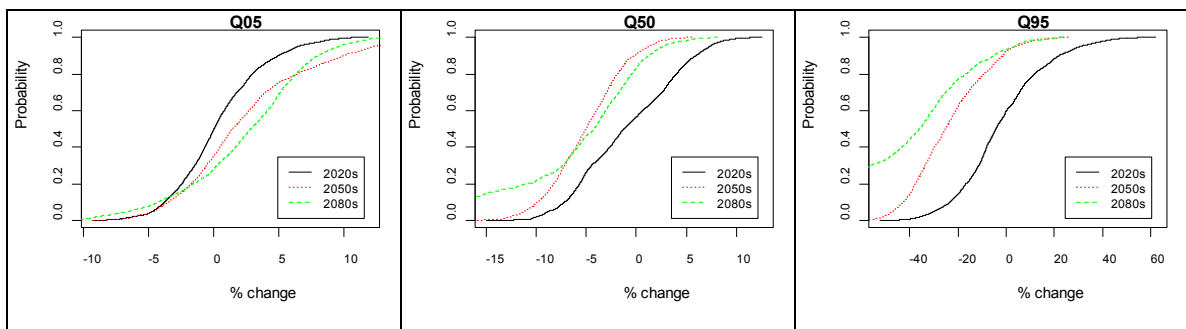

Figure 5.17 Cumulative distribution functions of percent changes in annual flow percentiles for the Maurmatta catchment

Projected changes in the frequency of low flow events for the Maurmatta catchment are illustrated in Figure 5.18. Model simulations suggest an increase in the frequency of low flow days for each future time horizon with increases of 7.27, 19.45 and 31.7 days projected for the 2020s, 2050s and 2080s respectively. On a seasonal basis the greatest increase in the number of Q95 days is projected to occur for the summer (18.47) over the 2080s horizon. Uncertainty ranges are also largest for this season, particularly over the 2080s, with model projections ranging from a reduction of almost nine days per year to an increase of up to 45 days. The spring also exhibits a notable increase in low flow days for the same horizon (8.95) with uncertainty bounds again spanning a sign change (-9.84 to +27.74).
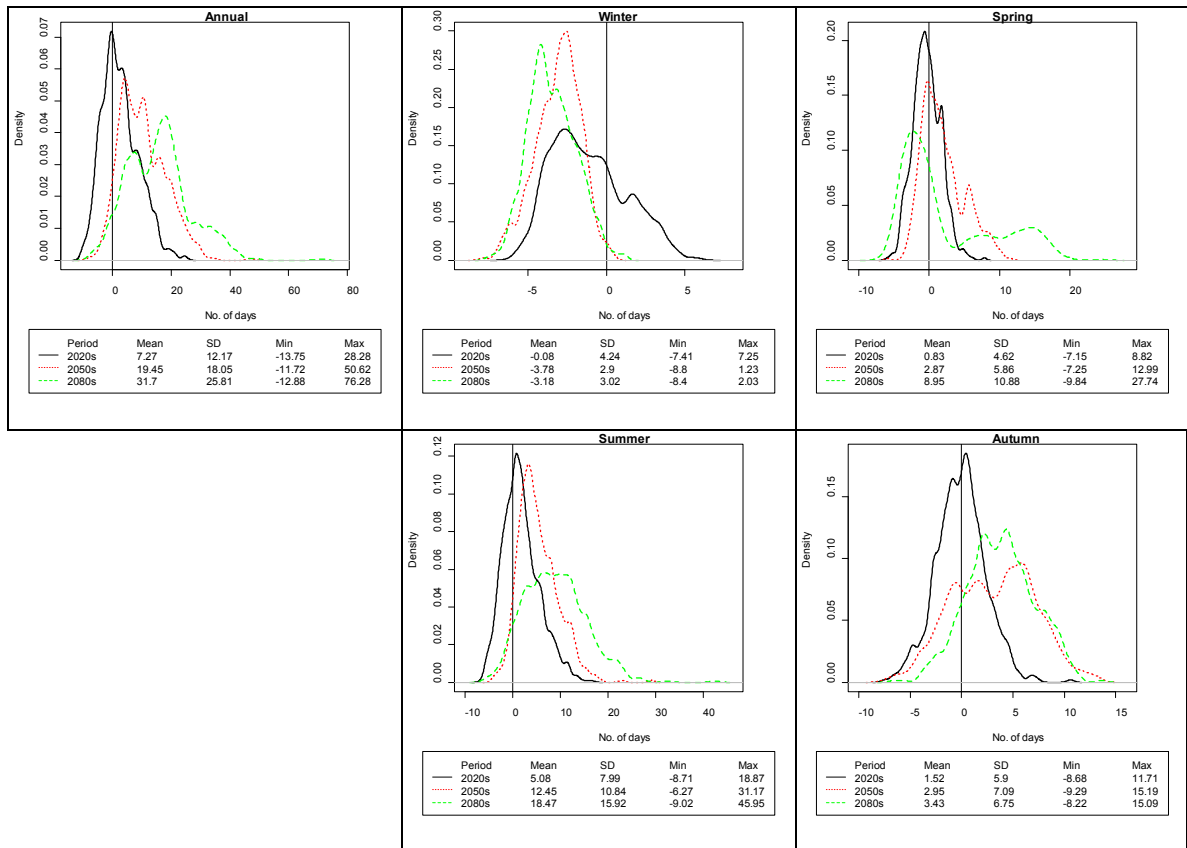
Figure 5.18 Simulated changes in the frequency of low flow events on an annual and seasonal basis for each future time period in the Maurmatta catchment
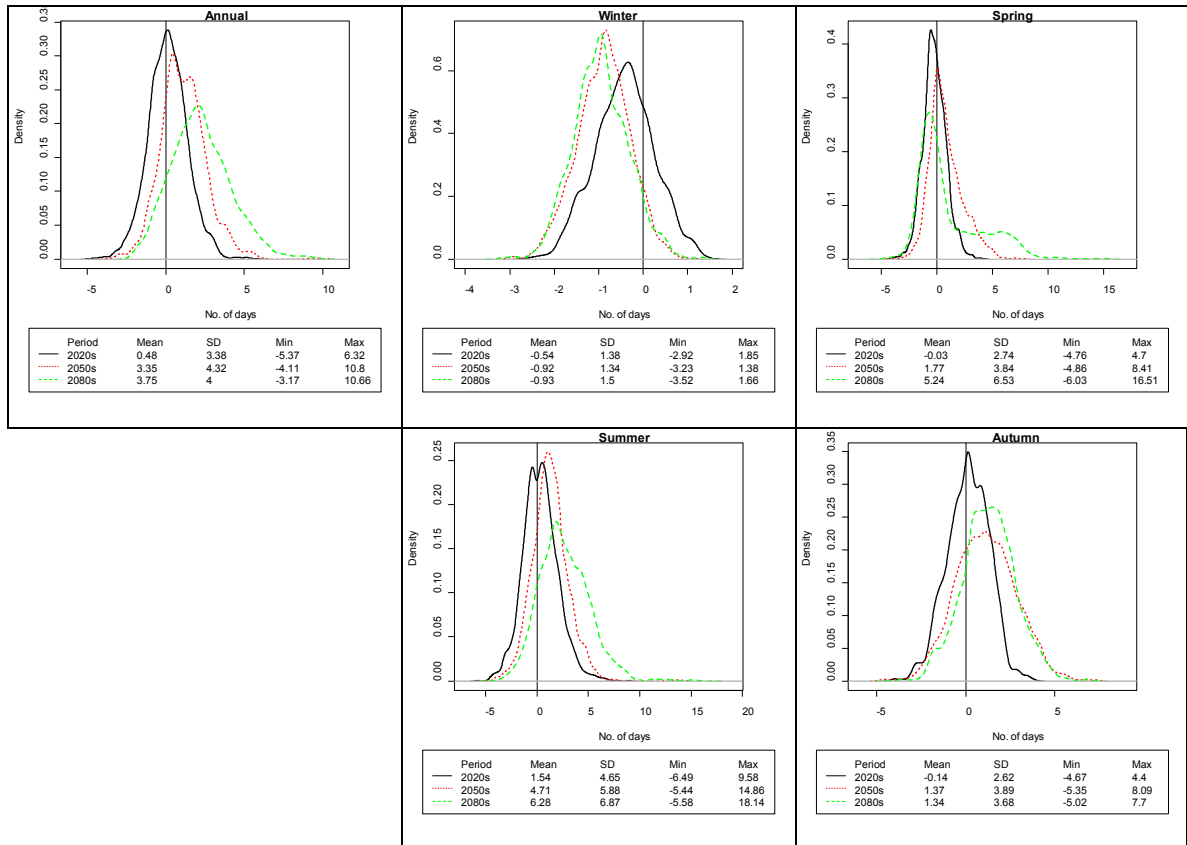

Figure 5.19 Simulated changes in the duration of low flow events on an annual and seasonal basis for each future time period in the Maurmatta catchment.

Figure 5.19 depicts the simulated changes in the duration of low flow events for the Maurmatta catchment. An average increase in the duration of low flow events of approximately three days is suggested by the end of the century. However model runs returned a maximum increase of almost 11 days. On a seasonal basis the greatest increases are associated with spring (+5.24) and summer (+ 6.28) for the 2080s.

5.10.4 Altahoney Catchment

Projected changes in the monthly mean flow regime for the Altahoney catchment are displayed in Figure 5.20. For the 2020s there is no clear indication of any changes in the flow regime outside the bounds of reference variability. The seasonality of the streamflow regime begins to become more pronounced by the 2050s with significant changes in catchment discharge returned for the months of December, May and September. By the 2080s the seasonality of the flow regime is projected to become heightened further. Increases in January and December are deemed to be significant when considered against baseline conditions whilst decreases in catchment discharge are significant for September. For the remaining months model simulations are not considered to be significant. Projections for the month of March display the widest uncertainty bounds with model runs ranging from -75% to +25%.
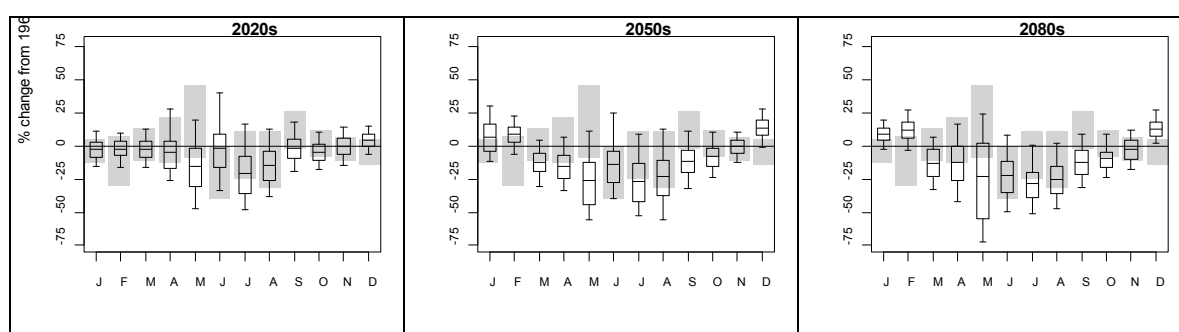

Figure 5.20 Changes in the monthly flow regime for the Altahoney catchment for the 2020s, 2050s and 2080s relative to the control period 1961-90.

Changes in the full range of flow conditions for the Altahoney over each future time horizon are examined using the following flow percentiles: Q05, Q50 and Q95. The cumulative distribution functions in Figure 5.21, constructed using the combined model simulations, depict the simulated changes for each percentile. Model projections suggest an increase in extreme high flows is likely with their occurrence becoming more frequent as the century progresses. A decrease in low flows is also suggested.
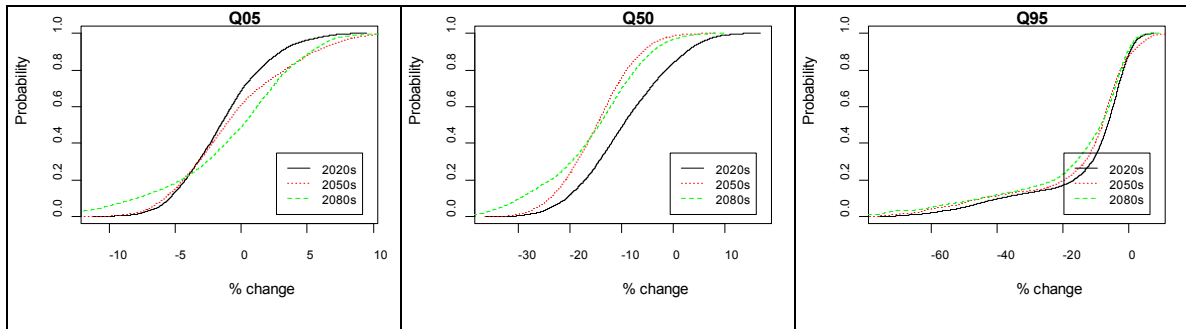
283

Figure 5.21 Cumulative distribution functions of percent changes in annual flow percentiles for the Altahoney catchment

Changes in the frequency of low flow events for the Altahoney catchment are presented in Figure 5.22. The results indicate an increase in the frequency of low flow events over each future period - with increases of 12.22, 11.23 and 28.17 days being returned for the 2020s, 2050s and 2080s respectively. On a seasonal basis the greatest increase in the number of low flow days is projected for the summer (14.77) over the 2080s horizon. The range in model projections are largest for this season, particularly the 2080s, with changes ranging from a reduction of almost sixteen days per year to an increase of up to 52 days. The spring also exhibits a notable increase in low flow days for the same horizon (+10.28) with uncertainty bounds again spanning a sign change (-10.55 to +31.12).
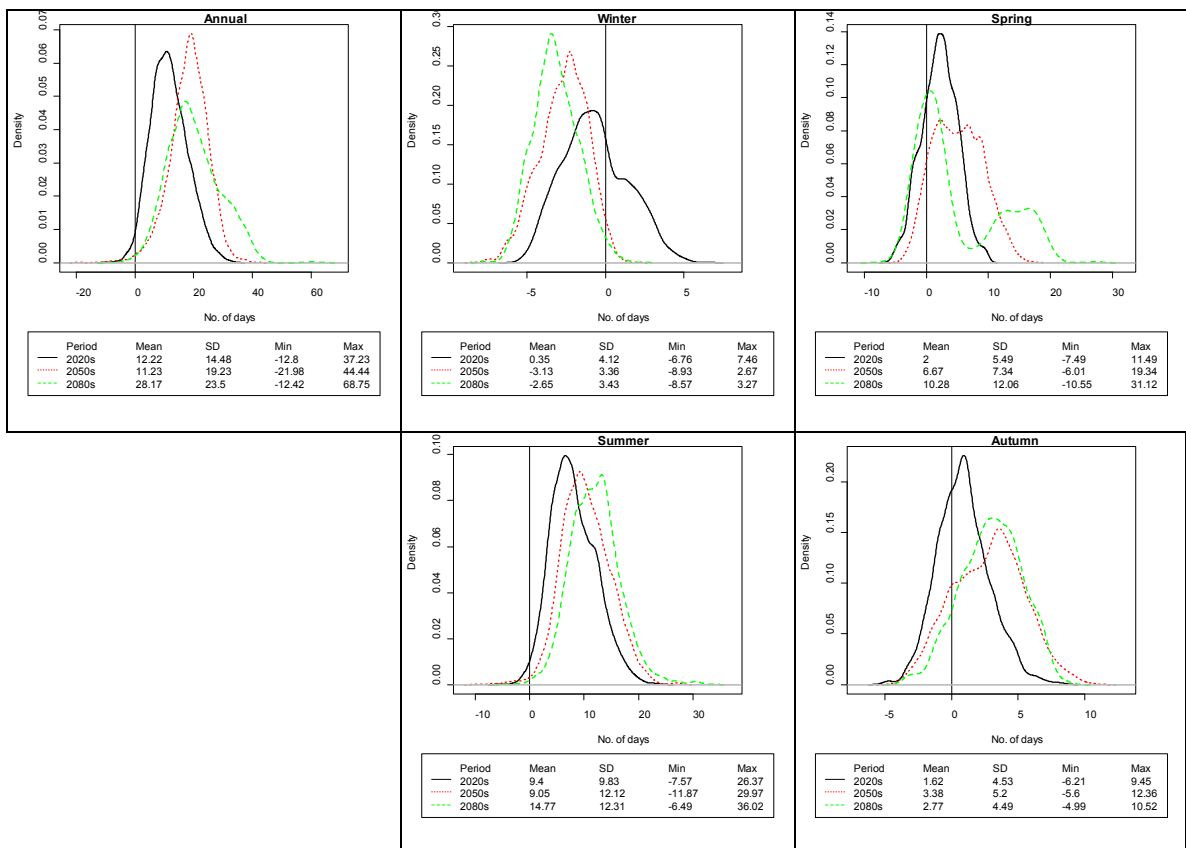

Figure 5.22 Simulated changes in the frequency of low flow events on an annual and seasonal basis for each future time period in the Altahoney catchment

Figure 5.23 depicts the simulated changes in the duration of low flow events for the Altahoney catchment. The duration of low flow events is calculated using the cumulative number of days for which average streamflow is below the Q95 threshold. On an annual basis an average increase in the duration of low flow events of approximately four days is suggested by the end of the century. The greatest increases in the average duration of Q95 flow conditions, on a seasonal basis, are shown for spring (+ 3.06) and summer (+ 5.42) over the 2080s. However the maximum increase returned by model simulations was much higher, over 14 days in both instances.
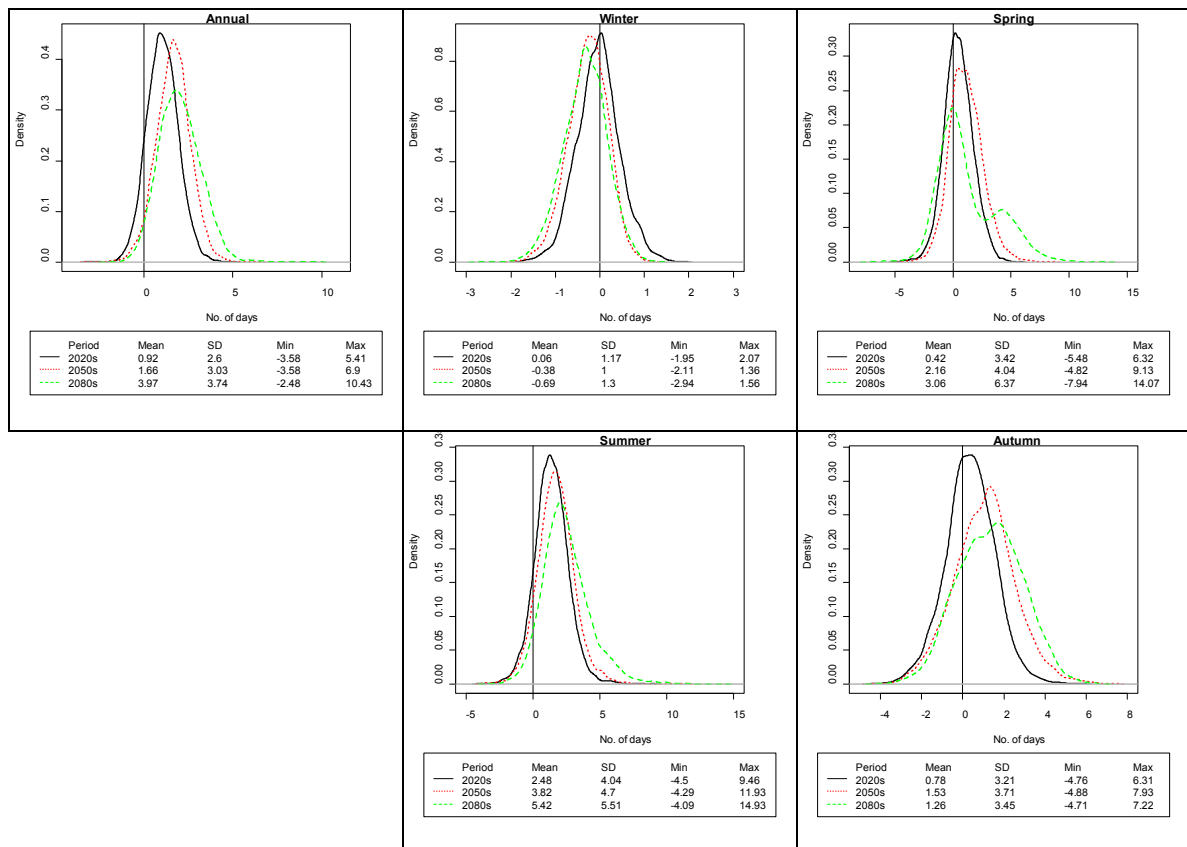

Figure 5.23 Simulated changes in the duration of low flow events on an annual and seasonal basis for each future time period in the Altahoney catchment

Table 5.13 displays the projected changes in the frequency of selected flood events for each future time period. For each future time period the greatest increases in frequency are derived from the CGCM2 GCM which projects a consistent decrease in the return period for all flood events over each time horizon. On the other hand a reduced frequency of occurrence of the selected flood events is suggest by the CSIRO A2 and B2 runs and Hadley A2 runs for the 2020s and 2050s. However, by the end of the century all runs with the exception of CSIRO model suggest and increase in the frequency of selected flood events. In the most extreme

case (HadCM3-B2) the current flood with a return period of 50 years is likely to occur once every 8.24 years by the 2080s.

Table 5.13 Changes in the frequency of selected flood recurrence intervals from the control period for each future time period for the Altahoney catchment.

2020s	CGCM2-A2	CGCM2-B2	CSIRO-A2	CSIRO-B2	HADCM3-A2	HADCM3-B2
t2	1.98	3.04	1.80	2.41	1.64	1.84
t5	3.79	5.80	4.73	7.72	3.53	4.55
t10	6.16	8.21	10.09	17.12	6.75	8.95
t15	7.93	10.14	15.62	25.72	10.43	13.42
t20	9.54	11.68	21.41	35.19	14.12	17.50
t50	16.53	16.63	56.96	88.44	37.51	41.52
2050s	**CGCM2-A2**	**CGCM2-B2**	**CSIRO-A2**	**CSIRO-B2**	**HADCM3-A2**	**HADCM3-B2**
t2	1.71	2.31	2.42	1.55	2.0	1.70
t5	2.74	3.66	8.15	3.22	6.67	3.34
t10	4.07	4.70	19.42	6.20	16.16	5.42
t15	5.06	5.50	31.59	9.02	27.92	7.22
t20	6.00	6.06	44.66	12.23	40.20	8.71
t50	10.036	7.82	129.92	31.90	122.97	15.92
2080s	**CGCM2-A2**	**CGCM2-B2**	**CSIRO-A2**	**CSIRO-B2**	**HADCM3-A2**	**HADCM3-B2**
t2	2.37	2.49	1.61	1.82	1.36	1.59
t5	3.59	4.20	3.51	4.47	2.68	2.76
t10	4.81	5.55	7.28	10.31	4.58	3.95
t15	5.58	6.59	11.55	15.75	6.39	4.84
t20	6.26	7.39	16.35	22.05	8.00	5.51
t50	8.68	9.82	52.14	61.60	15.68	8.24

5.10.5   Goulan Catchment

Figure 5.24 displays the projected changes in the mean monthly flow regime for the Goulan catchment. As the results for each month are within the bounds of reference variability model simulations indicate no clear change in monthly flows over the 2020s. By the 2050s the picture is a little clearer with some indication of a shift towards an increase in the seasonality of the streamflow regime. Changes for the months of March, July, September and October are significant outside reference variability. Over the 2080s horizon the exhibited pattern of increased seasonality remains largely the same as under the 2050s with decreases in flow now being significant for the months of March, July, August, September and October. As opposed to the other catchments considered none of the winter months display any significant increase in mean streamflow.
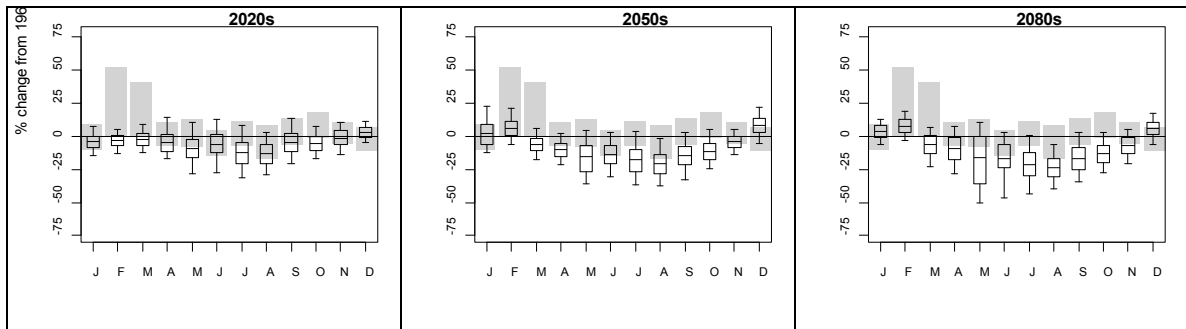
Figure 5.24 Changes in the monthly flow regime for the Goulan catchment for the 2020s, 2050s and 2080s relative to the control period 1961-90

Changes in the distribution of flow conditions for each future horizon were determined by analysing projected changes in the Q05, Q50 and Q95 flow percentiles. From Figure 5.25 model simulations suggest that an increase in high flows is likely, becoming more extreme by the end of the century. A decrease in low flows is also suggested similarly becoming more pronounced as the century progresses.
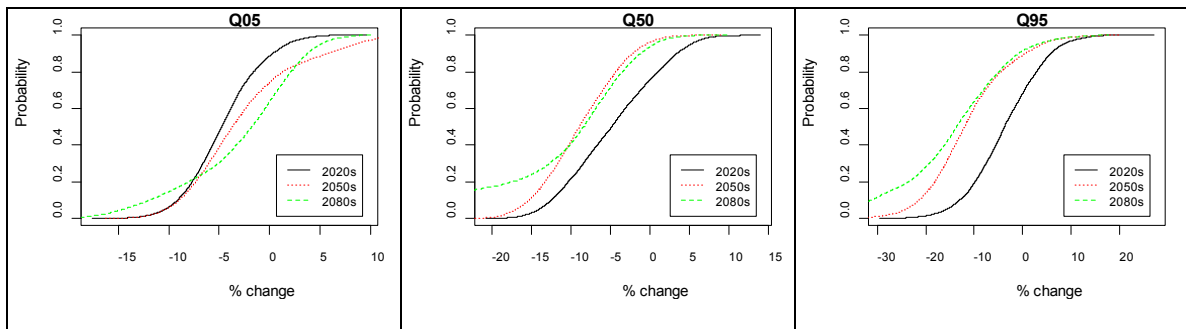

Figure 5.25 Cumulative distribution functions of percent changes in annual flow percentiles for the Goulan catchment

Changes in the frequency of low flow events for the Goulan catchment are displayed Figure 5.26. Projected changes in the number of days for which flows fall below this threshold, relative to the baseline period, are quantified for each future horizon. Model simulations suggest an increase in the frequency of low flow events for each horizon - with increases of 8.27, 12.32 and 37.88 days projected for the 2020s, 2050s and 2080s respectively. On a seasonal basis the greatest increase in the number of low flow days is projected to occur for the summer (19.7) over the 2080s. Uncertainty ranges are also largest for this season, particularly for the 2080s, with model simulations ranging from a reduction of almost 16 days per year to an increase of up to 56. Spring and autumn also exhibit a notable shift in the average occurrence of low flows with an increase of 11.58 and 8.42 respectively for the 2080s.
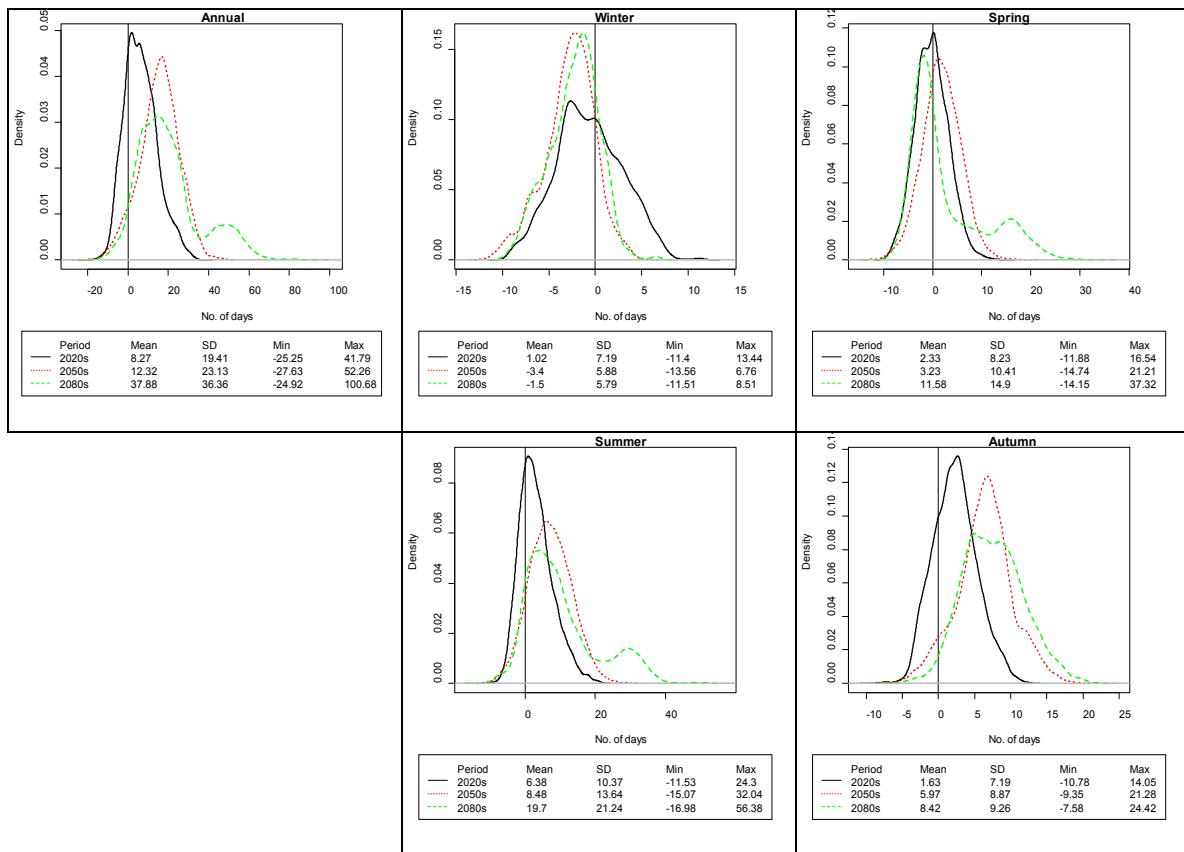
287

Figure 5.26 Simulated changes in the frequency of low flow events on an annual and seasonal basis for each future time period in the Goulan catchment.

Figure 5.27 depicts the simulated changes in the duration of low flow events. On an annual basis an increase in the duration of low flow events is evident for the each future horizon with increases of 2.38, 6.97 and 12.14 days for the 2020s, 2050s and 2080s respectively. The greatest increases in the duration of low flows are shown for spring and summer by the end of the century, with the latter showing an increase of over 20 days in the average duration of low flow conditions. Models simulations vary around this considerably with future model runs for this period ranging from -6.85 to +48.19.
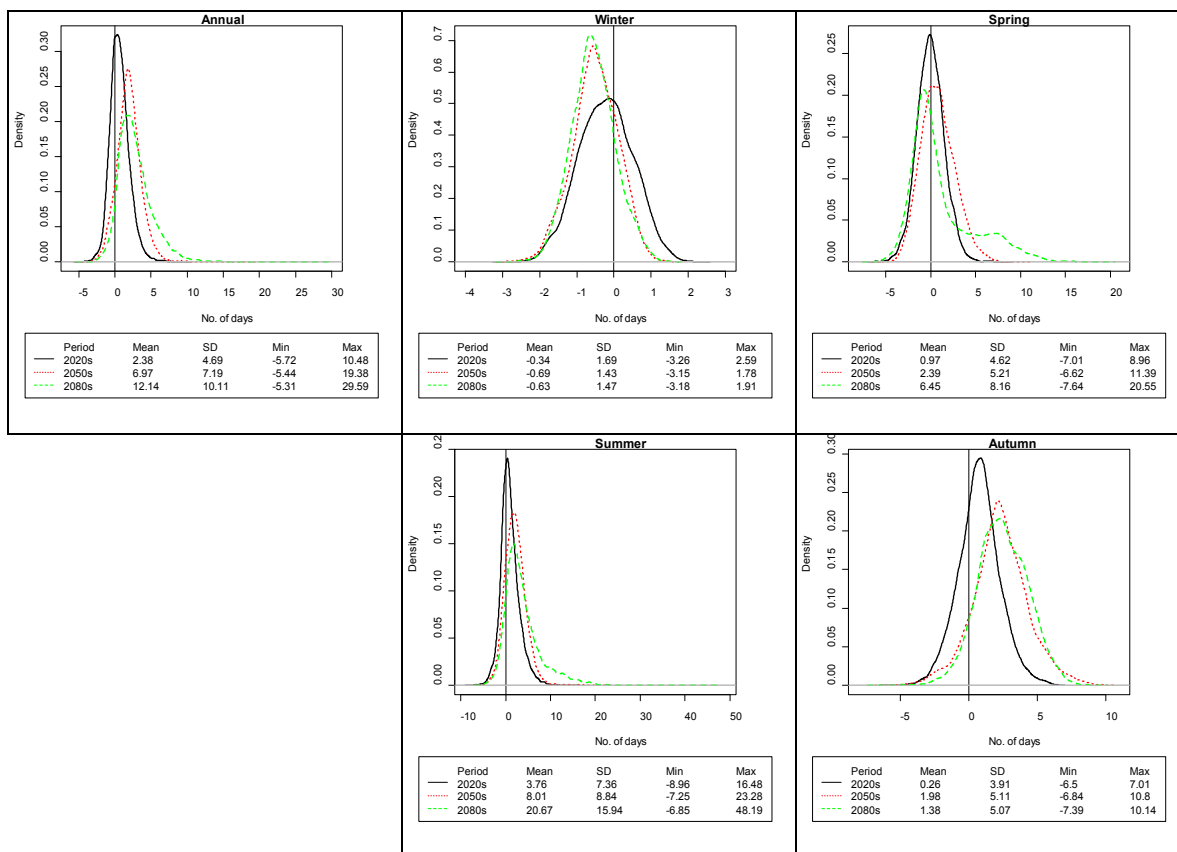
Figure 5.27 Simulated changes in the duration of low flow events on an annual and seasonal basis for each future time period in the Goulan catchment

Table 5.14 shows the projected changes in the frequency of selected flood events for each future time horizon. For each period the greatest in the frequency of flooding events of a given magnitude are derived from the CGCM2 GCM. Using the output from this model hydrological simulations suggest a consistent decrease in the return period for all flood events over each time horizon. Conversely a reduction in the frequency flooding events is suggested by the CSIRO A2 and B2 as well as the Hadley A2 for the 2020s and 2050s. However, by the end of the century all runs with the exception of CSIRO model suggest and increase in the frequency of selected flood events. In the most extreme case (HadCM3-B2) the current flood with a return period of 50 years is likely to occur once every 8.24 years by the 2080s.

Table 5.14 Changes in the frequency of selected flood recurrence intervals from the control period for each future time period

2020s	CGCM2-A2	CGCM2-B2	CSIRO-A2	CSIRO-B2	HADCM3-A2	HADCM3-B2
t2	2.71	3.07	1.67	2.51	1.82	1.78
t5	4.49	6.94	3.84	7.63	4.39	4.66
t10	7.91	11.56	7.37	18.73	9.20	10.65
t15	11.15	16.17	10.80	29.91	13.92	17.45
t20	13.99	20.14	13.70	42.71	19.29	25.71
t50	28.73	38.13	31.47	129.88	51.40	101.73
2050s	**CGCM2-A2**	**CGCM2-B2**	**CSIRO-A2**	**CSIRO-B2**	**HADCM3-A2**	**HADCM3-B2**
t2	1.62	2.11	2.05	1.46	2.36	1.72
t5	2.63	3.97	6.79	2.61	9.3	3.85
t10	3.77	6.16	18.68	4.96	24.35	7.26
t15	4.73	8.35	34.82	7.31	39.84	10.44
t20	5.51	10.25	51.96	10.05	57.79	13.77
t50	9.04	19.01	229.81	29.92	165.45	35.02
2080s	**CGCM2-A2**	**CGCM2-B2**	**CSIRO-A2**	**CSIRO-B2**	**HADCM3-A2**	**HADCM3-B2**
t2	2.33	2.48	1.45	1.68	1.40	1.61
t5	3.81	5.17	2.85	3.78	2.82	3.15
t10	5.17	8.49	5.49	7.94	5.36	5.02
t15	6.17	11.91	8.43	11.85	7.72	6.43
t20	6.93	14.93	11.16	16.11	10.30	7.74
t50	9.93	29.25	31.98	42.36	24.17	13.97

5.10.6 Srahrevagh Catchment

Projected changes in the monthly mean flow regime for the Srahrevagh catchment are displayed in Figure 5.29. For the 2020s there is no clear indication of any change in the flow regime outside the bounds of reference variability. The seasonality of the streamflow regime begins to become more pronounced by the 2050s with significant changes in catchment discharge returned for the months of September and December. By the 2080s the seasonality of the flow regime, it is suggested, will be enhanced further. Increases in December are deemed to be significant whilst decreases in streamflow are shown to be significant for August and September. For the remaining months model simulations are not considered to be significant.
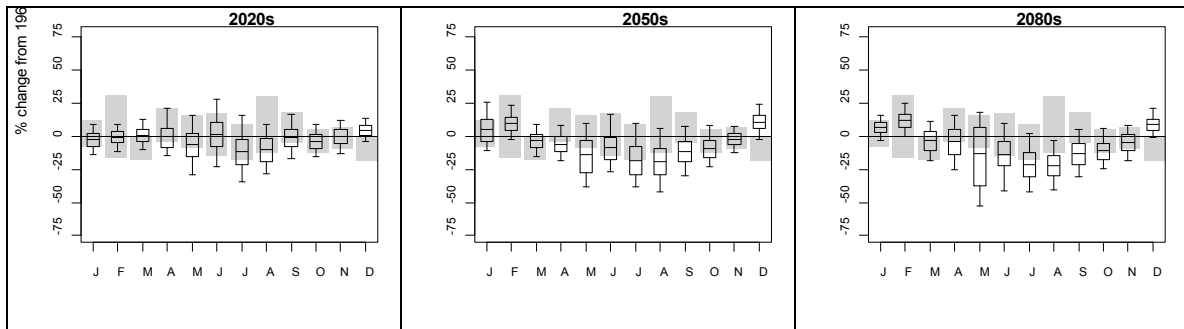
Figure 5.29 Changes in the monthly flow regime for the Srahrevagh catchment for the 2020s, 2050s and 2080s relative to the control period 1961-90.

Changes in the full range of flow conditions for the Srahrevagh over each future time horizon are examined using: Q05, Q50 and Q95. The cumulative distribution functions in Figure 5.30 display the model simulated changes for each percentile. Projections suggest a decrease in extreme low flows is likely with their occurrence becoming more frequent as the century progresses. Also noteworthy is the projected increase in Q05 flows.
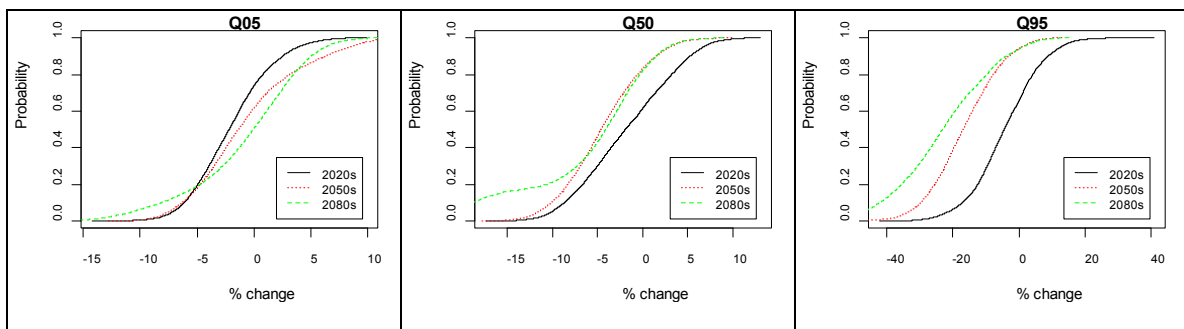

Figure 5.30 Cumulative distribution functions of percent changes in annual flow percentiles for the Srahrevagh catchment

Model returned changes in the frequency of Q95 flow events for the Srahrevagh catchment are displayed Figure 5.31. Model simulations suggest an increase in the frequency of low flow events for future period - with increases of 9.18, 19.95 and 29.27 days projected for the 2020s, 2050s and 2080s respectively. On a seasonal basis the greatest increase in the number of low flow days is projected to occur for the summer (18.95) over the 2080s. Uncertainty ranges are also largest for this season, particularly for the 2080s, with model simulations ranging from a reduction of almost 12 days per annum to an increase of up to 50. Spring and autumn also exhibit a notable shift in the average occurrence of low flows with an increase of 8.17 and 5.4 for the 2080s respectively.
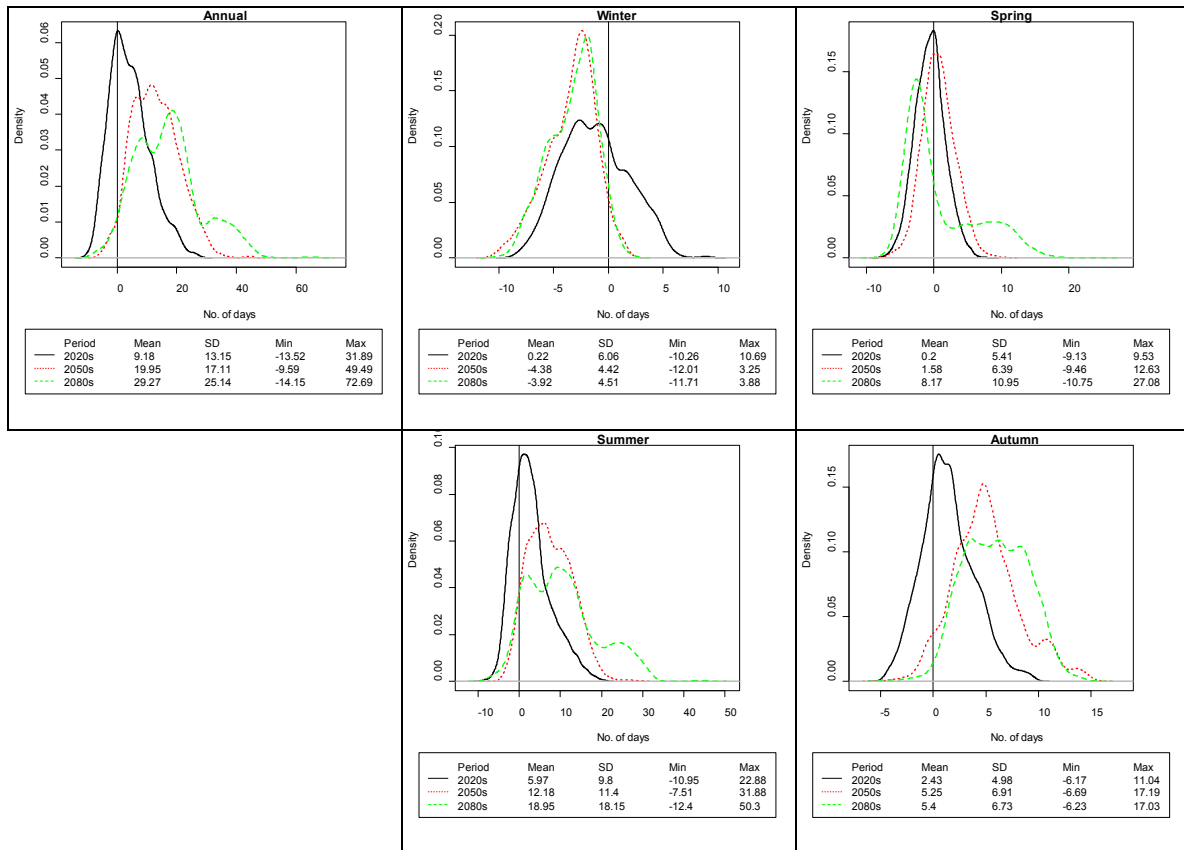
Figure 5.31 Simulated changes in the frequency of low flow events on an annual and seasonal basis for each future time period in the Srahrevagh catchment

Figure 5.32 depicts the simulated changes in the duration of low flow events. On an annual basis an increase in the duration of low flow events is evident for the each future horizon with increases of .59, 3.3 and 2.63 days for the 2020s, 2050s and 2080s respectively. The greatest increases in the duration of low flows conditions are returned for spring and summer over the 2080s, with the latter showing an increase of over 7 days.
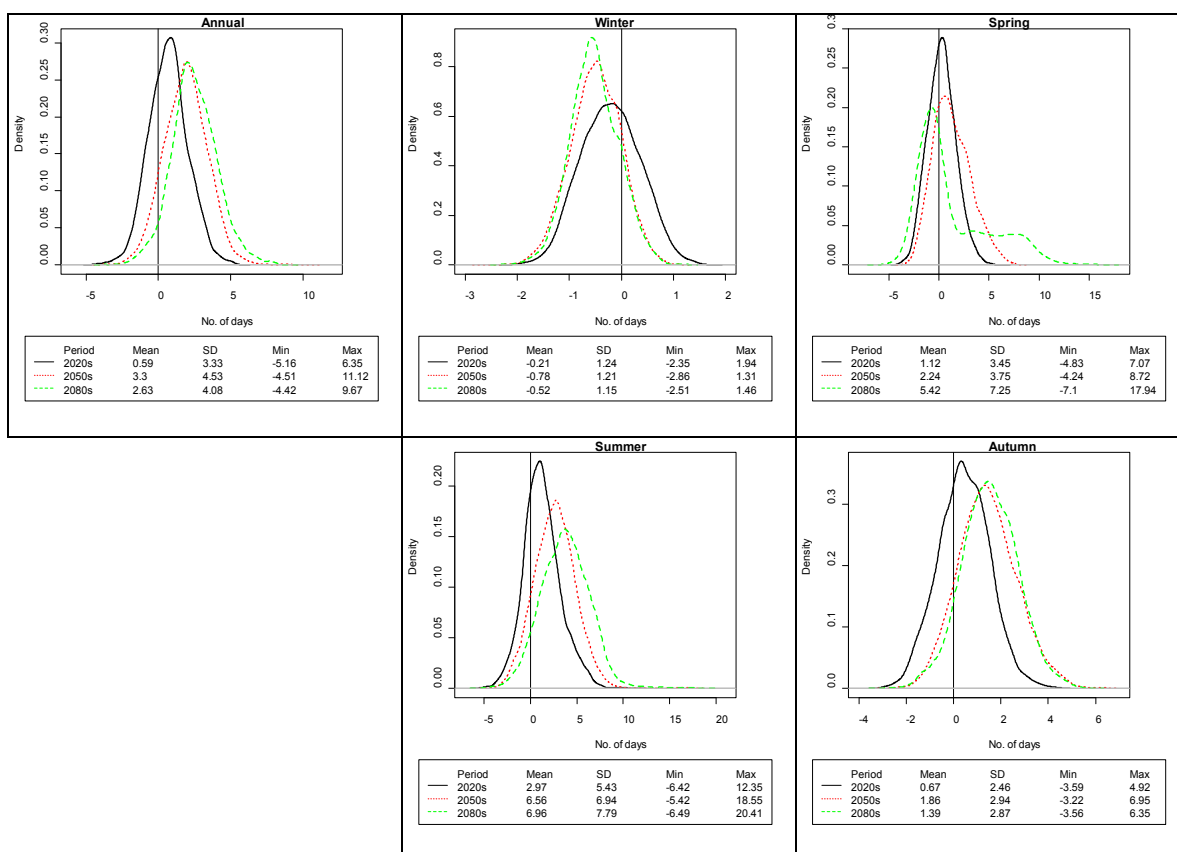
Figure 5.32 Simulated changes in the duration of low flow events on an annual and seasonal basis for each future time period in the Srahrevagh catchment.

Table 5.14 displays the projected changes in the frequency of selected flood events for each future time period. Model simulations which employed climate data from the CGCM2 GCM project a decrease in the return period for all flood events over each time horizon. A reduced frequency of occurrence for a number of flood events is suggest by the CSIRO A2 and B2 models as well as the Hadley A2 GCM for the 2020s and 2050s. However, by the end of the century all runs with the exception of CSIRO model suggest a decrease in the return period for all events of a given magnitude. In the most extreme case (CGCM2-A2) the current flood with a return period of 50 years is likely to occur once every 7.08 years by the 2080s.

Table 5.14 Changes in the frequency of selected flood recurrence intervals from the control period for each future time period

2020s	CGCM2-A2	CGCM2-B2	CSIRO-A2	CSIRO-B2	HADCM3-A2	HADCM3-B2
t2	1.98	2.91	1.71	2.42	1.71	1.71
t5	3.94	5.73	3.96	7.41	3.80	4.28
t10	6.73	8.17	7.34	16.53	7.31	9.19
t15	8.55	10.35	10.62	26.27	10.97	13.52
t20	10.22	12.35	13.83	35.41	14.23	18.87
t50	19.32	19.63	29.94	98.26	37.03	49.76
2050s	CGCM2-A2	CGCM2-B2	CSIRO-A2	CSIRO-B2	HADCM3-A2	HADCM3-B2
t2	1.62	2.16	2.13	1.49	2.14	1.67
t5	2.52	3.70	6.87	2.79	7.68	3.47
t10	3.66	5.01	16.10	5.07	19.56	6.13
t15	4.37	6.18	26.82	7.48	33.74	8.11
t20	5.00	7.26	38.66	9.76	47.41	10.29
t50	8.26	11.17	114.49	26.01	158.33	20.24
2050s	CGCM2-A2	CGCM2-B2	CSIRO-A2	CSIRO-B2	HADCM3-A2	HADCM3-B2
t2	2.21	2.33	1.48	1.72	1.39	1.53
t5	3.36	4.22	2.85	4.12	2.68	2.80
t10	4.48	5.87	5.10	8.51	4.67	4.30
t15	5.08	7.35	7.48	13.24	6.58	5.27
t20	5.57	8.71	9.97	17.71	8.18	6.24
t50	7.08	13.69	24.47	49.14	17.84	9.93

5.11 Implications for the Catchment

For any given catchment system changes in local climate conditions have the potential to fundamentally alter key aspects of their hydrological cycle including the generation of surface runoff, groundwater recharge, evapotranspiration rates and the dynamics of groundwater-surface water interactions. In the context of this study the impact of climate change on the streamflow regime of each catchment was assessed. A flow regime describes the average seasonal behaviour of flow and encompasses the timing, size and duration of flow events in a river system. Flow regimes influence the morphology of river channels, biodiversity and key processes which sustain the aquatic ecosystem. In this regard maintaining a 'natural' flow regime is essential to the ecological health and overall well being of a catchment system. Any alterations in climate therefore have potentially far-reaching implications not just for flow conditions but for other aspects of the catchment which are directly and indirectly linked to this. Outlined below are some of the key findings for the catchments included in this study

followed by a number of general conclusions which can be made regarding the impact climate change is likely to have on the Burrishoole system as a whole.

Due to the projected increase in winter precipitation average streamflow is expected to increase by up to 25% for the months of January and/or December for all catchments over the period 2069-2099. For the month of June reductions of up to 40% were returned for three of the selected catchments (Glendahurk, Maurmatta and Goulan). Accompanied by this is a suggested decrease in mean flow of between 15 – 40% for the months of September, October and August variously across all catchments. A reduction in the return period for flooding events is expected for each catchment, the most extreme of which are associated with the Glendahurk, Altahoney and Goulan with exhibited reductions in the return period of a 50 year event to between 7 and 9 years by the 2080s. Model simulations indicate an increase in extremely low summer flow for each catchment, an outcome which is commensurate with the projected decreases in summer precipitation. For all catchments, by the 2080s, model simulations suggest an increase in the number of extreme low flows days (≤Q95) of between 13 and 20%. Associated with this is an increase of between 4 and 7 days in the consecutive number of days for which flows are equal to or below the Q95 threshold for all catchments during the summer season. Model simulations suggest that the incidence of summer low flows will increase as the century progresses.

Given the similarity of their physical characteristics (e.g. soil type, land-use, etc.) model simulations for each catchment were shown to largely agree in terms of both the timing and magnitude of projected changes in their respective flow regimes. This aspect of the model results allows robust inferences to be made about the overall response of the Burrishoole system to changes in local climate conditions and the implications this may have for its aquatic environment as well as the overall management of the catchment itself.

A number of general conclusions can be made regarding key changes in the streamflow hydrology of the Burrishoole system under the conditions of future climate forcing.

- Model simulations suggest an amplification of the seasonal flow regime for all catchments (i.e. higher winter flows accompanied by lower summer flows) with this underlying trend becoming more pronounced as the century progresses.
- A shift in mean flow (Q50) conditions for a number of months was found with projected changes being deemed significant (i.e. outside the bounds of natural variability under baseline climate conditions) over the 2050s and to a greater extent

the 2080s. Simulated changes in mean monthly flows over the 2020s were found not to be significant with regards to reference variability.

- An increase in the incidence of extreme low flows (Q95), most notably during the summer and spring seasons, is projected. Associated with this is a suggested increase in the average number of consecutive days for which flows are equal to or below the Q95 threshold. Low flow events are anticipated to become more frequent through the latter half of the century.

- An increase in the occurrence of peak discharge events, characterized using the Q05 flow threshold, is projected. Associated with this is a reduction in the return period for flooding events. Model simulations suggest the frequency of extreme high flows will increase as the century progresses.

As noted by Krasovskaia and Gottschalk (2002) the characteristics of a catchments flow regime are dependent on the climate and physiographic features of the drainage area. Advancing this it can be said that the characteristics of any catchment play a central role in determining its capacity to exacerbate or mitigate changes in streamflow arising from alterations in local climate conditions. The response of the Burrishoole catchment to projected changes in the local precipitation regime, embodied by the principal findings from this study outlined above, can be linked to the physical attributes of the system itself.

The climate scenarios developed for the Burrishoole catchment suggest an increasing tendency towards a more distinct seasonal precipitation regime leading to wetter winters and drier summers with this trend likely to become more pronounced over the latter part of the century. In catchments whose hydrological regime is significantly influenced by groundwater flow increased winter receipts can be beneficial by recharging groundwater stores to a higher level and thus providing ample baseflow with which to sustain river levels during drier periods of the year. Essentially groundwater dominated catchments have the capacity to store the additional rainfall received during the winter for release during the drier summer months. The Burrishoole system however does not possess the storage properties required to moderate the influence of an increasingly seasonal rainfall regime. The catchment is underlain by relatively unproductive aquifers limiting its overall groundwater storage capacity. This feature of the Burrishoole system leaves it vulnerable to the anticipated changes in its precipitation regime, a fact underlined by the suggested increase in the occurrence of extreme low flows especially during the drier summer months.

The topography of each catchment, along with the dominance of blanket peat, promotes the rapid transmission of rainfall received over the drainage area to the stream network. This aspect of the Burrishoole's hydrological system impedes groundwater recharge and contributes to the 'flashy' nature of the flow response to precipitation events. In essence the Burrishoole system lacks the capacity to buffer or dampen the flood causing potential of heavy rainfall events suggesting it is sensitive to more intense precipitation events. This assertion is backed-up by the projected increase in the frequency of high flow and flooding events under changing climate conditions.

Of specific interest in this study are the impacts of a changing flow regime on the catchments capacity to sustain and nurture indigenous stocks of Atlantic salmon. As hydrological conditions are of fundamental importance to the well being of salmonid fish anticipated changes in different components of the natural flow regime, including mean and extreme conditions, have wide ranging implications for Atlantic salmon populations in the Burrishoole catchment.

It is known that each component of the natural flow regime (e.g. high, mean and low flows) play an important role in different aspects of the salmon's life cycle. Spates are required for fish migration while flooding events are beneficial for de-silting spawning gravels and contribute to the overall maintenance of the stream network. Low and medium flows control the amount of available habitat and have a significant influence on fish migration. As pointed out by Gilvear et al. (2002) hydrology determines not only the physical habitat in which salmon live but the organisms on which they feed, who themselves are also dependent on flow conditions. This alludes to the multiple direct and indirect relationships which exist between river flow and salmonid populations.

Outlined below are the potential impacts of climate induced alterations in different aspects of a flow regime for each life stage of the Atlantic salmon as presented by Walsh and Kilsby (2007).

Spawning and Egg Deposition
- An increase in flash flooding could lead to the wash out of eggs laid in gravels.
- A sudden decrease in flows levels could leave redds stranded out of water before fertilization or after preventing the emergence of fry.
- Higher flows may lead to increased sediment loads which could cause the siltation of redds.
- The reduced availability of spawning habitat caused by decreased or increased flows.

297

Alevins

- An increase in flow velocity could lead to the displacement of newly emerged salmon downstream.
- *Juvenile Salmon*
- Successive reduced flow years may have a detrimental effect on salmon stocks, taking years to recover.

Smolts, Migration and Returning Salmon

- Wetter Springs may induce earlier migration of smolts to sea which may reduce survival capacity in the marine environment.
- A reduction in the number of spates may hamper the upstream migration of returning fish.
- Rapid reductions in flow may lead to stranding of migratory salmonids.

5.12 Summary

To assess the potential impacts of climate change on the Burrishoole catchment system a conceptual rainfall-runoff model was employed to simulate streamflow under the forcing conditions of future climate using scenarios derived from grid-scale GCM output. To account for the uncertainty associated with local-scale estimates of future climate change the output from three GCMs (HadCM3, CSIROmk2 and CGCM2), each run under both the A2 and B2 SRES emission scenarios, were downscaled using two different regression-based methods. Flow conditions for each of the five selected sub-catchments which comprise part of the greater Burrishoole catchment system, along with the adjacent Glendahurk catchment, were modelled using the downscaled climate scenarios. To address the uncertainty associated with identifying optimum parameter values an ensemble of equally plausible parameter sets were used when modelling future conditions for each catchment. Model projections were considered over three future time horizons (2020s, 2050s and 2080s) relative to the standard baseline period (1961-1990). To determine whether simulated changes could be correctly attributed to an anthropogenically induced shift in local climate conditions the natural variability of the flow regime under 'current' and future climate was explicitly considered when interpreting results.

Given the similarity of each of the six selected catchments, in terms of their physiographic features, their response to changing climate conditions is taken to be representative of changes in the hydrology of the Burrishoole system as a whole. This is defensible given the correspondence shown between the model results for each individual catchment. Generally model simulations suggested an increasing tendency towards a more distinct seasonal

streamflow regime across the catchment with higher flows occurring in winter (DJF) and lower flows during the summer (JJA) and autumn (SON). This is commensurate with predicted changes in the catchments precipitation regime. Increased winter flows coupled with the fast response time of the Burrishoole system leave it vulnerable to more intense precipitation events. This manifests itself in a projected decrease in the return period for peak discharge and flooding events. Also suggested is an increase in summer and spring low flows. In general the results suggest a greater deviation from reference conditions, for both mean and extreme flows, as the century progresses with changes being more acute under the A2 emission scenario when compared to the less carbon intensive B2 scenario.

Any alterations in the prevailing flow conditions, or what can be taken as the 'natural' flow regime, have significant implications for the well-being of the Burrishoole catchments aquatic ecosystem including its capacity to sustain and nurture Atlantic salmon populations. All aspects of a river systems streamflow regime, including extreme flows, play an important role at each stage in the salmon's life cycle. However a more extreme flow regime, as is suggested by model projections, has the potential to significantly disrupt the habitat conditions required to sustain salmon populations and allow them to successfully complete different stages in their life cycle. In this regard understanding the implications of a climate induced shift in the flow regime is important when devising future management strategies and making policy decisions for the catchment.

The Burrishoole system remains relatively untouched by human activity and as such future management will present unique challenges as reducing the human impact (e.g. removing impoundments and modifications, greater control on pollution, reducing abstractions) on it will not play as great a role in mitigating the long term effects of climate change when compared with other catchments which have been subjected to significant human interference. Managing the catchment will essentially require adaptation to and mitigation of a shift in the 'natural' flow regime which will be difficult given the physical characteristics of the catchment itself. Future management strategies may look at altering land-use practices across the catchment or examine the possibilities for micro-managing different aspects of the stream channels themselves, including their morphology and riparian zones, with a view to sustaining optimal habitat conditions (e.g. spawning grounds) for Atlantic salmon populations.

5.13 Key Findings

- Projected changes in streamflow for each catchment were found to be relatively similar with no one catchment exhibiting deviations from the general trend in changing flow conditions found across the Burrishoole system. This is indicative of the relatively similar physical characteristics presented by each catchment.

- Given the dominant role runoff plays in shaping each catchments hydrology, projected changes in streamflow conditions are predominantly driven by, and are sensitive to, alterations in the local precipitation regime (i.e. wetter winters and drier summers).

- An increase in the seasonality of the flow regime (i.e. higher winter flows and lower summer flows) is projected for all catchments with this underlying trend becoming more pronounced as the century progresses.

- Changes in mean flows for each month over the 2020s were deemed to lie within the bounds of natural variability for the baseline period and thus could not be clearly attributed to the underlying climate change 'signal'. This is a finding common to all selected catchments.

- By the 2050s model simulations suggest a clear shift in mean flow conditions outside reference variability for some months. The most consistent changes across each catchment were found for to occur for the winter (DJF) and autumn (SON) months. Comparatively fewer significant changes for the spring (MAM) and summer (JJA) months were found.

- Over the 2080s mean monthly flows deviate further from baseline conditions and as such projected changes for a greater number of months were deemed to be significant with regards to baseline variability. Significant increases in mean flow for the months of January and December, accompanied by decreases for the months of June, October and August, are suggested for the majority of catchments.

- The incidence of extreme low flows, defined using the Q95 flow threshold, is anticipated to increase during the summer and spring seasons with this trend becoming more pronounced through the latter part of the century.

- A reduction in low flows is accompanied by an increase in the average number of consecutive days for which streamflow is equal to or less than the Q95 threshold. This was found to be most extreme for the spring and summer seasons over the 2080s.

- Model simulations indicate an increase in high flows (Q05) as the century progresses with deviations from reference conditions being most apparent over the latter half of the century.

- Although there is a degree of inter-model variability regarding the projected return period for flooding events it is generally evident that the occurrence of floods will

increase. This is a finding common to each catchment and is more extreme under the A2 emissions pathway.

- The absence of any significant storage capacity across the Burrishoole system suggests that it is unable to provide any natural means of flow regulation which could moderate the impact of an increasingly seasonal rainfall regime on flow conditions - thereby leaving the catchment vulnerable to changes in local climate. This is illustrated by the projected increase in low flows during the summer months when baseflow is required to sustain river levels.

- The 'flashy' nature of the streamflow response to precipitation events, a trait exhibited by all catchments, highlights the inability of each system to buffer or dampen the impact of heavy rainfall on peak discharge. This alludes to the sensitivity of the catchment to any intensification in its rainfall regime under future climate forcing, a point underlined by the projected increase in high flow and flooding events.

- Projected changes in the flow regime for the Burrishoole catchment have potentially significant implications for the catchments aquatic ecosystem including its capacity to sustain and nurture Atlantic salmon populations.

- Management of the catchment will require explicit consideration of the likely impacts climate change will have on its hydrological regime.